Annu. Rev. Nucl. Part. Sci. 2002. 52:23–63
doi: 10.1146/annurev.nucl.52.050102.090713

PION-NUCLEUS INTERACTIONS*

T.-S. H. Lee
Physics Division, Argonne National Laboratory, Argonne, Illinois 60439; e-mail: lee@theory.phy.anl.gov

R. P. Redwine
Department of Physics and Laboratory for Nuclear Science, Massachusetts Institute of Technology, Cambridge, Massachusetts 02139; e-mail: redwine@mit.edu

Key Words elastic, inelastic, absorption

PACS Codes 25.80.−e, 24.10.−i, 24.50.+g

■ **Abstract** Pion-nucleus interactions have been extensively investigated in the past three decades with the meson factories at LAMPF, TRIUMF, and PSI. This article gives a pedagogical review of the advances and discusses open questions as well as issues related to current research.

CONTENTS

1. INTRODUCTION

As the lightest meson, the pion has long been known to play a critical role in the interactions between nucleons. In fact, the nucleon-nucleon (*NN*) interaction at distances larger than about 0.7 fermi (fm) is well described in terms of the

exchange of pions. This means that, although we believe that the ultimate theory of the strong interactions is quantum chromodynamics (QCD) with quark and gluon degrees of freedom, much of the strongly interacting matter in the universe (nuclei) is best described in terms of nucleons and mesons. Therefore, it is of fundamental importance to understand as quantitatively as possible the complicated but common situation in which a pion interacts with a nucleus. It is for this reason that the three so-called meson factories [the Los Alamos Meson Physics Facility (LAMPF) in New Mexico, United States; the Paul Scherrer Institute (PSI) in Villigen, Switzerland; and the Tri-University Meson Facility (TRIUMF) in Vancouver, Canada] were constructed. We now have a wealth of data on pion-nucleus interactions. Correspondingly, there has been much progress in theoretical understanding of these data, and conventional nuclear theories have been advanced to account for pionic and some other non-nucleonic degrees of freedom.

In addition to the intrinsic interest, what has been learned about pion-nucleus interactions is also important to many other high-priority efforts in nuclear physics. With the Thomas Jefferson National Accelerator Facility and the accelerators at MIT-Bates and at Mainz, we are now able to use electron scattering to study the nucleus and its components in regions of energy and momentum that challenge traditional models of nuclei and may lead to understanding of the transition to quark/gluon degrees of freedom. We are also now seeing, with the Relativistic Heavy Ion Collider (RHIC) and eventually the Large Hadron Collider (LHC), extensive data from collisions of heavy nuclei that may show explicit evidence of the transition from a nucleon/meson system to a quark-gluon plasma. Clearly, it is critical to both of these general efforts to understand quantitatively the interactions of the lightest meson, the pion, with nuclei under a variety of conditions, as such understanding will be the starting point for exploring new physics as well as interpreting the data obtained.

The pion is a spin-0 boson with isospin $I = 1$. It has three charged states (π^+, π^0, π^-) and can have charge-exchange reactions with the nucleon: $\pi^- p \rightarrow \pi^0 n$ and $\pi^+ n \rightarrow \pi^0 p$. The high-quality data obtained at meson factories are mainly in the region where the pion kinetic energy T_π is less than about 300 MeV. In this energy region, the pion-nucleon (πN) total cross section exhibits a pronounced resonant peak at $T_\pi \sim 180$ MeV with a width of about 120 MeV. It has been well established that this is due to the formation of the spin $J = 3/2$ and isospin $I = 3/2$ $\Delta(1232)$ resonance. The overall pion-nucleus interaction in this energy region also appears to be strongly influenced by the Δ resonance. This is evident from the pion-nucleus total cross sections (1), shown in Figure 1. The resonance peak shifts to lower energy and the width becomes broader as nuclear mass increases.

For much of the energy region in question, the total pion-nucleus cross section is very large (comparable to nuclear geometric size), and an incoming pion would be expected to interact mainly with the nucleons near the nuclear surface. In general, one expects the following processes to be possible in pion-nucleus interactions: elastic scattering, where the target nucleus is left in its ground state; inelastic scattering, where the outgoing pion leaves the nucleus in an excited state; charge exchange, either single or double, which is a special case of inelastic scattering;

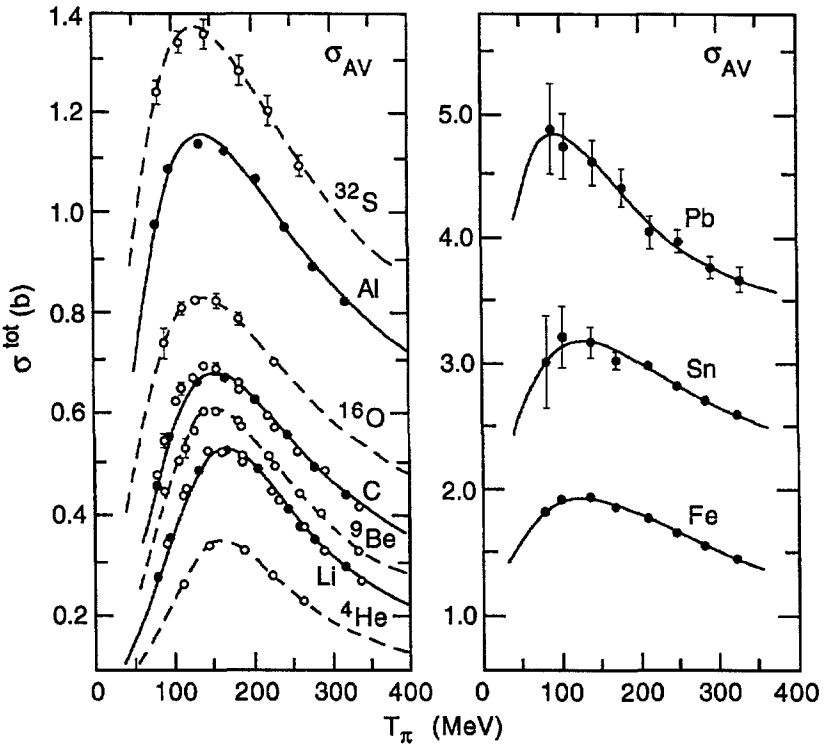

Figure 1 Pion-nucleus total cross sections averaged over the pion charge. The curves are from empirical fits to the data assuming a Breit-Wigner resonant shape. The results are from Reference 1.

and absorption, where no pion emerges. Double charge exchange and absorption have no analog with most other traditional nuclear probes. They allow the pion to probe special nuclear properties and interactions.

The most fundamental question in the study of pion-nucleus interactions is how each of these reactions contributes to the total cross sections shown in Figure 1. This question could not be answered before the meson factories started to produce high-precision data for each reaction channel. Earlier pion-nucleus experiments suffered from the low intensity of pion beams and poor energy resolution. The separation of nuclear final states was often difficult. With the extensive data from meson factories, we now have a good understanding of the dynamical content of the pion-nucleus total cross section. For example, the energy dependence and nuclear mass (A)–dependence of each of the reaction channels have been measured, as shown in Figures 2 and 3. This review includes pedagogical discussions of our current understanding of each reaction channel.

This article does not cover πN and πNN interactions; we refer the reader to the review by Garcilazo & Mizutani (2). The earlier work on pion-nucleus interactions was well reviewed by Koltun (3). In this review, we focus on the advances since

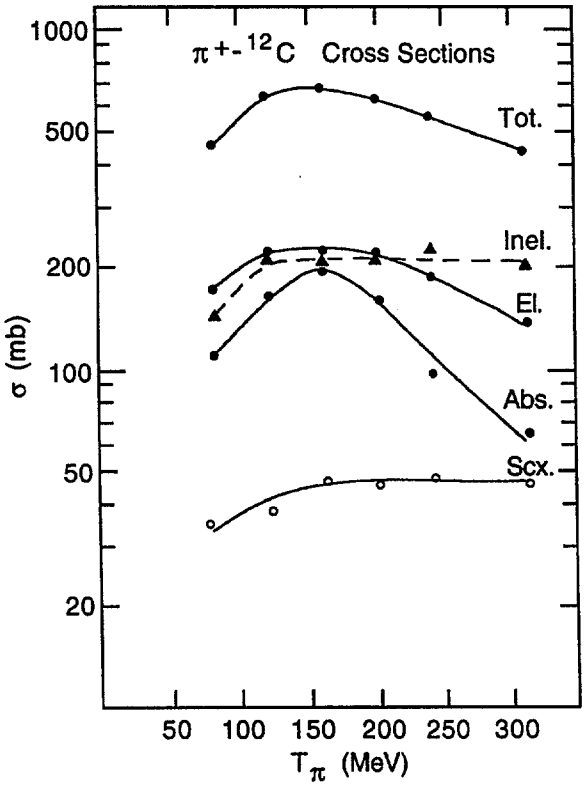

Figure 2 Decomposition of the π^+ ^{12}C total cross sections (Tot.) into the contributions from elastic scattering (El.), inelastic scattering (Inel.), absorption (Abs.), and single charge exchange (Scx.). T_π is the pion kinetic energy. The results are from Reference 180. The curves are only for guiding the eye.

the meson factories started to operate in the mid 1970s. There have been several noteworthy reviews of this and related areas of pion physics (4–7).

The very extensive list of publications on pion-nucleus interactions cannot all be cited in this short article. We include only the references most closely related to our discussions here.

In Section 2, we review the theoretical models of pion-nucleus reactions that have been applied to interpret the experimental data. We discuss pion-nucleus elastic scattering in Section 3, and inelastic scattering, including charge-exchange processes, in Section 4. The important pion absorption reactions are discussed in Section 5. In Section 6, we address issues related to current research.

2. THEORETICAL MODELS

Most theoretical work on pion-nucleus interactions is based on extensions of the well-established nuclear many-body theory to include π and Δ degrees of freedom.

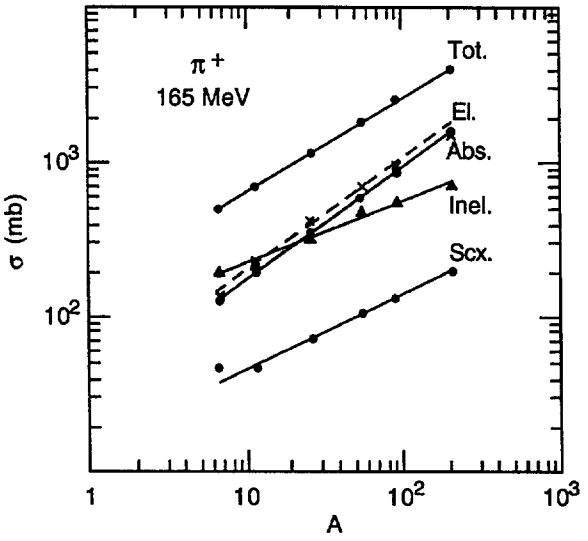

Figure 3 Nuclear mass (A)–dependence of pion-nucleus interaction cross sections at 165 MeV. The labels for displayed data are identical to those in Figure 2. The data are from Reference 180. The curves are only for guiding the eye.

In this review, we focus on the results obtained through approaches based on either multiple scattering theory (8, 9) or the Δ-hole model (10–13). The approaches based on semiclassical formulations (such as those given in References 14–17) are not discussed.

It is instructive to begin by enumerating the basic one-nucleon and two-nucleon mechanisms of all possible pion-nucleus reaction channels indicated in Figures 2 and 3. The most economical way to account for the Δ-resonance excitation is to introduce a vertex interaction $h_{\pi N \leftrightarrow \Delta}$ that can convert a πN state into a Δ, as illustrated in Figure 4*a*. This vertex interaction can generate πN scattering via the $\pi N \rightarrow \Delta \rightarrow \pi N$ transition. The πN scattering can also be due to the non-Δ interaction $v_{\pi N}$, such as the one-particle-exchange mechanisms illustrated in Figure 4*b*. To account for pion absorption, the excited Δ must be allowed to interact with the surrounding nucleons. The lowest-order absorption mechanism is due to a $\Delta N \rightarrow NN$ transition, as illustrated in Figure 4*c*. Pion absorption can also be due to the non-Δ mechanism $F_{\pi NN \leftrightarrow NN}$, as illustrated in Figure 4*d*.

In the following two subsections, we briefly describe how the multiple scattering formulation and the Δ-hole model accomodate the reaction mechanisms illustrated in Figure 4.

2.1. Multiple Scattering Formulation

The multiple scattering approach is based on a Hamiltonian of the following form:

$$H = K_\pi + H_A + \sum_i V_{\pi N}(i), \qquad 1.$$

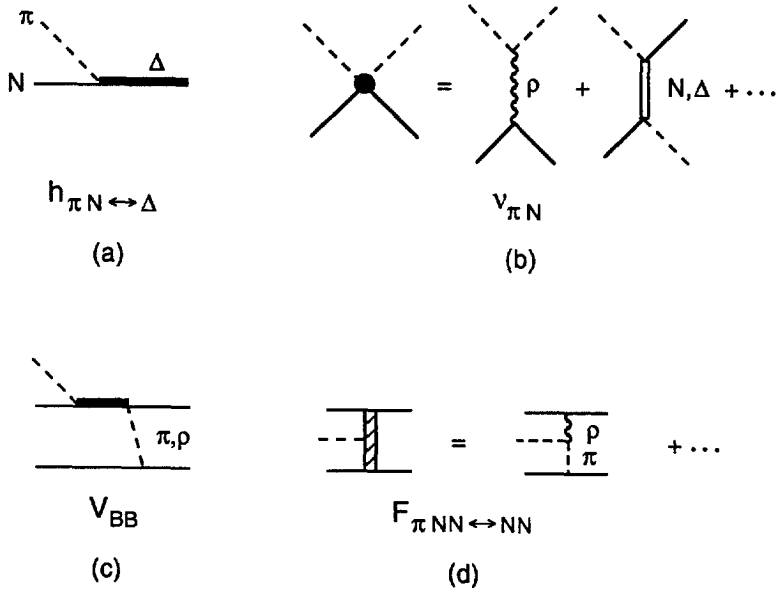

Figure 4 Graphical representations of some basic mechanisms of pion-nucleus interactions.

where K_π is the pion kinetic energy operator, $V_{\pi N}$ is a πN potential, and H_A is the conventional nuclear Hamiltonian for A nucleons. The Δ degree of freedom is not treated explicitly and the resonant scattering $\pi N \to \Delta \to \pi N$ is included in $V_{\pi N}$. Clearly, the scattering formulation based on this Hamiltonian will not include pion absorption via either the Δ excitation $\pi NN \to N\Delta \to NN$ (Figure 2*c*) or the nonresonant absorption mechanism $F_{\pi NN \to NN}$ (Figure 2*d*). Furthermore, the medium effects on Δ propagation cannot be accounted for. This is the intrinsic deficiency of the multiple scattering approach. Thus, some phenomenological procedures are needed to adjust the multiple scattering formulation to achieve a satisfactory description of the data.

The multiple scattering formulation is aimed at describing the pion-nucleus scattering processes in terms of an in-medium πN scattering matrix defined by the following equation:

$$\tilde{t}_i(E) = V_{\pi N}(i) + V_{\pi N}(i)\,\frac{1}{E - K_\pi - H_A + i\epsilon}\,\tilde{t}_i(E). \qquad 2.$$

Note that $\tilde{t}(E)$ is a many-body operator because the propagator contains the nuclear Hamiltonian H_A.

Let us first consider the scattering processes for which the initial and final nuclear states Φ_a are eigenstates defined by $H_A|\Phi_a\rangle = E_a|\Phi_a\rangle$. The projection operator for the subspace spanned by these states is denoted by P. It is then

straightforward to apply the projection operator technique (9, 18) to derive, from the Hamiltonian equation (Equation 1) and the definition (Equation 2) for $\tilde{t}$, the following pion-nucleus scattering equation:

$$T_{ab}(E) = U_{ab}(E) + \sum_c U_{ac}(E) \frac{P}{E - K_\pi - H_A + i\epsilon} T_{cb}(E), \qquad 3.$$

where (a, b, c) denote the states in the subspace P. The driving term of Equation 3 can be calculated perturbatively from the in-medium scattering matrix $\tilde{t}$:

$$U_{ab}(E) = \langle \Phi_a | U^{(1)}(E) + U^{(2)}(E) + \cdots | \Phi_b \rangle. \qquad 4.$$

Only the first-order and second-order terms in the right-hand side of Equation 4 have been investigated. Explicitly, they are

$$U^{(1)}(E) = \frac{(A-1)}{A} \sum_i \tilde{t}_i(E), \qquad 5.$$

$$U^{(2)} = \frac{(A-1)^2}{A^2} \sum_{ij} \tilde{t}_i(E) \frac{Q}{E - K_\pi - H_A - U^{(1)}(E) + i\epsilon} \tilde{t}_j(E), \qquad 6.$$

where $Q = 1 - P$. Note that the propagator in Equation 6 now also contains the first-order potential $U^{(1)}$.

Because of the many-body nature of the operator $\tilde{t}(E)$, the evaluations of $U^{(1)}$ and $U^{(2)}$ are very difficult. In practice, they are most commonly evaluated by using the impulse approximation. This amounts to assuming that $\tilde{t}(E) \sim t(\omega)$, where the free πN scattering t-matrix is a one-body operator defined by

$$t(\omega) = V_{\pi N} + V_{\pi N} \frac{1}{\omega - K_N - K_\pi + i\epsilon} t(\omega). \qquad 7.$$

Here ω is an appropriately chosen πN collision energy. The matrix element of $U^{(1)}$ defined by Equation 5 can then be written as

$$U^{(1)}_{ab}(\vec{k}', \vec{k}, E) = (A-1) \int d\vec{p}\, \rho_{ab}(\vec{p} - \vec{q}, \vec{p}) \langle \vec{p} - \vec{q}, \vec{k}' | t(\omega) | \vec{p}, \vec{k} \rangle, \qquad 8.$$

where $\vec{k}$ and $\vec{k}'$ are the pion momenta and $\vec{q} = \vec{k}' - \vec{k}$. The nuclear transition dynamics is contained in

$$\rho_{ab}(\vec{p}, \vec{p}\,') = \int d\vec{p}_2 \cdots d\vec{p}_A \Phi^*_a(\vec{p}, \vec{p}_2 \cdots \vec{p}_A) \Phi_b(\vec{p}\,', \vec{p}_2 \cdots \vec{p}_A). \qquad 9.$$

The evaluation of Equation 8 is further simplified by using the factorization approximation. It is assumed that the πN t-matrix in the right-hand side of Equation 8 can be evaluated at a fixed nucleon momentum $\vec{p} = \vec{p}_0$. The t-matrix element can then be removed from the integration and the familiar fixed-scatterer-approximation (FSA) form is obtained:

$$U^{\mathrm{FSA}}_{ab}(\vec{k}', \vec{k}, E) = \langle \vec{k}', \vec{p}_0 - \vec{q} | t(\omega) | \vec{k}, \vec{p}_0 \rangle F_{ab}(\vec{q}), \qquad 10.$$

where $F_{ab}(\vec{q})$ is the nuclear transition form factor defined by

$$F_{ab}(\vec{q}) = \langle \Phi_a | \frac{1}{A} \sum_i e^{-i\vec{q}\cdot\vec{r}_i} | \Phi_b \rangle. \qquad 11.$$

The factorized form (Equation 10) resembles the forms used in electron scattering and high-energy hadron scattering. The only difference is in the projectile-nucleon amplitude. Thus the factorized form, despite its deficiency, is commonly used in analyzing data. Questions concerning the optimum choices of the fixed momentum $\vec{p}_0$ and collision energy ω for evaluating U^{FSA} have been extensively investigated (see Reference (19) for a review). Detailed studies of U^{FSA} can be found in References (20–29).

For investigating elastic scattering, we set $P = |\Phi_0\rangle\langle\Phi_0|$, with Φ_0 being the nuclear ground-state wavefunction. The scattering equation (Equation 3) then becomes the familiar Lippmann–Schwinger equation

$$T_{00}(E) = U_{00}(E) + U_{00}(E) \frac{1}{E - K_\pi - K_A + i\epsilon} T_{00}(E), \qquad 12.$$

where $U_{00}(E)$ is the optical potential defined by Equation 4. Most of the analyses of elastic scattering data were carried out by setting $U_{00}(E) = U_{00}^{\mathrm{FSA}}(E)$. This is certainly not sufficient for a detailed description of the data. It is most common to adjust the parameters of U^{FSA} to fit the data. An alternative is to include the second-order optical potential defined by Equation 6. Unfortunately, the calculation of the second-order optical potential is very complicated and involves less-well-understood two-body nuclear transition densities. Only very limited advances in this direction have been made (29–32). In practice, one observes that if the FSA is also used to evaluate Equation 6, the second-order optical potential is proportional to the square of nuclear density ρ. A similar ρ^2-dependence term is also expected if the two-body pion absorption effects, as illustrated in Figures 4*c* and 4*d*, are included. To account for the correlation effects and absorption effects within the multiple scattering theory, the compromise is to employ the following semi-phenomenological optical potential:

$$U_{00} \sim U_{00}^{(1)} + W\rho^2, \qquad 13.$$

where the first-order potential $U_{00}^{(1)}$ is calculated theoretically using the procedures outline above. In practice, the FSA form (Equation 10) is most commonly used for $U_{00}^{(1)}$ in Equation 13. The folded form (Equation 8) is also used in some investigations (28, 29). The strength W of the ρ^2 term of Equation 13 is determined phenomenologically by fitting both the total cross sections and integrated total elastic scattering cross sections. The well-known Ericson–Ericson potential (33) and Michigan State University (MSU) potential (34, 35) were also developed within this semi-phenomenological approach, using more sophisticated parameterizations of the ρ^2 terms (as described in Reference 36).

For inelastic scattering, it is most common to assume that the nuclear excitation is due to the mechanism that is first-order in $\tilde{t}$. Equation 3 is then reduced to the distorted wave impulse approximation (DWIA) form

$$T_{ab}(E) = \langle \chi^{(-)}_{a,E} | U^{(1)}_{ab}(E) | \chi^{(+)}_{b,E} \rangle. \tag{14.}$$

The pion scattering wavefunctions in the above equation obey

$$|\chi^{(\pm)}_{a,E}\rangle = \left[1 + \frac{1}{E - K_A - K_\pi \pm i\epsilon} T_{aa}(E)\right] |\chi_E\rangle, \tag{15.}$$

where $|\chi_E\rangle$ is a plane wave state. If the FSA (Equation 10) is used to evaluate the transition potential $U^{(1)}_{ab}$, then the DWIA amplitude (Equation 14) can have a simpler factorized form. In particular, if the nuclear shell model is used to evaluate the nuclear transition form factors, Equation 14 can be written as

$$T_{ab} = \sum_{\alpha,\beta} \langle \Phi_a | b^+_\alpha b_\beta | \Phi_b \rangle \langle \chi^{(-)}_{a,E} \phi_\alpha | t(\omega) | \chi^{(+)}_{b,E} \phi_\beta \rangle, \tag{16.}$$

where $b^+_\alpha (b_\alpha)$ is the creation (annihilation) operator for a nucleon with a single particle wavefunction ϕ_α.

The factored DWIA form, like Equation 16, is most widely used in investigating inelastic scattering and single-charge-exchange (SCE) reactions. It is also commonly used to investigate the nucleon knockout processes $(\pi, \pi' N)$. Here the wavefunction ϕ_α in Equation 16 is replaced by a scattering wavefunction $\phi^{(-)}_{a,E_N}$ calculated from an optical potential.

The DWIA form is also used for double-charge-exchange (DCE) reactions. Here the nuclear transition is described by $U^{(2)}$ of Equation 6. By inserting the relevant intermediate states c of the Q-space, we obtain the following matrix element:

$$\begin{aligned} U^{(2)}_{ab}(\vec{k}', \vec{k}, E) = (A-1)^2 \sum_c \int d\vec{k}_1 d\vec{k}_2 \\ U^{(1)}_{ac}(\vec{k}', \vec{k}_1, E) \langle \vec{k}_1 | \frac{1}{E - K_\pi - E_c - U^{(1)}_{cc}(E) + i\epsilon} | \vec{k}_2 \rangle \\ \times U^{(1)}_{cb}(\vec{k}_2, \vec{k}, E). \end{aligned} \tag{17.}$$

In some calculations, one further replaces $U^{(1)}_{cc}$ in the propagator by a constant $\bar{U}_0$ and uses the FSA $U^{(1)}_{ab} \sim U^{\mathrm{FSA}}_{ab}$ of Equation 10. Then the intermediate state c can be summed up by using closure:

$$U^{(2)}_{ab}(\vec{k}', \vec{k}, E) = \int d\vec{k}_0 \sum_{i,j} \langle \Phi_a | \frac{t_i(\vec{k}', \vec{k}_0, \omega_0) e^{i\vec{r}_i \cdot (\vec{k}' - \vec{k}_0)} t_j(\vec{k}_0, \vec{k}, \omega_0) e^{i\vec{r}_j \cdot (\vec{k}_0 - \vec{k})}}{E - E_\pi(k_0) - \bar{\epsilon} - \bar{U}_0} | \Phi_b \rangle. \tag{18.}$$

The inelastic scattering has also been studied by using the coupled-channel equations defined by Equation 3 with the simplification that $U_{ab} = U^{\mathrm{FSA}}_{ab}$. A

more refined calculation is to use the semi-phenomenological optical potential of the form of Equation 13 to describe the diagonal elements U_{aa}. The coupled-channel approach is most natural for investigating charge-exchange reactions involving only analog nuclear states. Some efforts have also been made to investigate coupled-channel effects, due to low-lying nuclear states, on inelastic scattering.

2.2. Δ-Hole Model

The Δ-hole model of pion-nucleus interactions is based on the observation that the nuclear dynamics at intermediate energies ($E_\pi \sim$ 80–300 MeV) is dominated by the formation of a Δ in nuclei. This is evident from the energy dependence of pion-nucleus total cross sections, as shown in Figure 1. The pion-nucleus interactions can therefore be more effectively described in terms of Δ variables.

In the Δ-hole model it is assumed that the pion-nucleus interactions can be described by the transitions between three subspaces defined by the projection operators P, D, and Q. The P-space is spanned by the basis states $\Psi_P = \chi_\pi \otimes \Phi_A$, D-space by $\Psi_D = \phi_\Delta \otimes \Phi_{A-1}$, and Q-space by $\Psi_Q = \Phi_A$, where Φ_A, χ_π, and ϕ_Δ are the wavefunctions for an A-nucleon system, the pion, and the Δ, respectively. The Hamiltonian in P-space is of the following form:

$$H_P = H_A + K_\pi + V_{\pi A}, \tag{19.}$$

where H_A is the Hamiltonian for an A-nucleon system, K_π is the free pion Hamiltonian, and $V_{\pi A}$ is the nonresonant pion-nucleus interaction, which does not involve Δ excitation. The Hamiltonian in D-space is

$$H_D = H_{A-1} + K_\Delta + V_\Delta, \tag{20.}$$

where K_Δ is the free Hamiltonian of the Δ and V_Δ represents the Δ interaction with the $(A-1)$ nucleons. The Hamiltonian in Q-space is

$$H_Q = H_A\,. \tag{21.}$$

The Δ-hole model is based on the doorway assumption that there is no interaction connecting P-space and Q-space:

$$H_{PQ} = H_{QP} = 0\,. \tag{22.}$$

The transition between P-space and D-space is defined by a $\Delta \rightarrow \pi N$ vertex interaction:

$$H_{PD} = H_{DP}^{+} = f_{\pi N\Delta}. \tag{23.}$$

By applying the standard projection operator technique (18), it is straightforward to obtain from the above definitions the transition matrix elements between the states in P-space. Let us consider the simplest case, in which the P-space only contains the ground state $|\Phi_0\rangle$ of the target nucleus. The resulting pion-nucleus

elastic scattering amplitude can be written as

$$T_{00}(\vec{k}', \vec{k}, E) = \langle \vec{k}' \Phi_0 | T(E) | \vec{k} \Phi_0 \rangle , \qquad 24.$$

where $\vec{k}$ is the pion momentum in the center-of-mass frame. The scattering operator in Equation 24 is defined by

$$T(E) = T_{\mathrm{bg}}(E) + T_{\Delta}(E) , \qquad 25.$$

where the nonresonant scattering operator T_{bg} is due to the nonresonant interaction $V_{\pi A}$ of the P-space Hamiltonian (Equation 19). In practice, the nonresonant amplitude T_{bg} is calculated from a simple FSA optical potential $U_{\mathrm{bg}} \sim t^{\mathrm{bg}}\rho$, where t^{bg} is the non-Δ part of the πN scattering amplitude and ρ is the nuclear density.

The resonant scattering operator in Equation 25 can be written as

$$T_{\Delta} = \Omega_{\mathrm{bg}}^{(-)\dagger}(E) f_{\pi N\Delta}^{\dagger} G_{\Delta}(E) f_{\pi N\Delta} \Omega_{\mathrm{bg}}^{(+)}(E) , \qquad 26.$$

where the pion scattering operators $\Omega_{\mathrm{bg}}^{(\pm)}(E)$ are determined only by the nonresonant optical potential U_{bg}. The Δ-nucleus interactions are contained in the propagator $G_{\Delta}(E)$. It is most convenient to perform the Δ-hole calculation using the independent-particle representations for the eigenstates of H_A and H_D. The Δ propagator can then be written as

$$G_{\Delta} = \frac{1}{D(E - H_D) - W^{\uparrow} - \Sigma_{\mathrm{Pauli}} - W_{\mathrm{sp}}}, \qquad 27.$$

where

$$D(\omega) = \omega - \Sigma_{\mathrm{free}}(\omega). \qquad 28.$$

The energy shift, $\Sigma_{\mathrm{free}}(\omega)$, is due to the Δ decay into a πN state and is defined by the vertex interaction $f_{\pi N\Delta}$,

$$\Sigma_{\mathrm{free}}(\omega) = \int k^2 dk \frac{|f_{\pi N\Delta}(k)|^2}{\omega - E_{\pi}(k) - E_N(k) + i\epsilon}. \qquad 29.$$

The term $W^{\uparrow}$ in Equation 27 describes the pion propagation that occurs while the nucleus remains in its ground state:

$$W^{\uparrow} = f_{\pi N\Delta}^{\dagger} \frac{P}{E - H_P} f_{\pi N\Delta}. \qquad 30.$$

Obviously, Equations 28 and 29 do not contain Pauli blocking effects on the Δ decay. This is corrected by the term Σ_{Pauli} in Equation 27. It is defined by

$$\Sigma_{\mathrm{Pauli}} = -f_{\pi N\Delta}^{\dagger} \frac{P'}{E - H_{P'}} f_{\pi N\Delta}. \qquad 31.$$

Here P' contains all of the occupied single nucleon states. The effect due to the coupling with the Q-space is contained in the so-called spreading potential W_{sp} of Equation 27. It accounts for the pion absorption effects due to, for example,

the two-body mechanisms illustrated in Figures 4*c* and 4*d*. On the other hand, multinucleon absorption mechanisms are possible; hence, the spreading potential W_{sp} is treated phenomenologically in most of the Δ-hole calculations.

Most of the Δ-hole model studies of inelastic scattering, including charge-exchange scattering and $(\pi, \pi' N)$ knockout reactions, were carried out using a formulation similar to the DWIA formulation described in the previous subsection. Such a formulation can be obtained by first observing that the elastic scattering amplitude T_{00} (Equation 24) can be equivalently calculated from the Lippman–Schwinger equation (Equation 12) with the pion-nucleus optical potential defined by

$$U_{00}(E) = \langle \Phi_0 | \sum_i \tau_i(E) | \Phi_0 \rangle. \tag{32.}$$

Here the medium-corrected πN t-matrix $\tau(E)$ is defined by

$$\tau_i(E) = t_i(E) - t_i(E) \frac{P'}{E - H_{P'}} \tau_i(E), \tag{33.}$$

where P' is defined as in Equation 31 and

$$t_i(E) = t_i^{bg}(E) + t_i^{\Delta}(E). \tag{34.}$$

Here t^{bg} is the nonresonant πN t-matrix, and the Δ absorption effects are included in the second term:

$$t^{\Delta}(E) = f^{\dagger}_{\pi N \Delta} \frac{1}{D(E - H_D) - W_{sp}} f_{\pi N \Delta}. \tag{35.}$$

Note that the second term in Equation 33 is to account for the Pauli blocking effect, which is crucial in the Δ-hole model. Equations 32–35 (derived in Reference 134) are completely equivalent to the derivation of Reference (133).

By using the optical potential U_{00} defined by Equation 32 to generate the distorted waves and replacing the free t-matrix $t(\omega)$ by $\tau(E)$ in Equations 16–17, one obtains formulations for investigating inelastic scattering within the Δ-hole model, including charge-exchange and $(\pi, \pi' N)$ knockout, as well as double-charge-exchange (DCE) reactions.

3. ELASTIC SCATTERING

Extensive data on pion-nucleus elastic scattering from a wide range of nuclei have been obtained at meson factories (37, 38, 41–78). The data in general show the characteristics of diffractive scattering. That is, minima in the elastic scattering angular distributions correspond to the diffractive minima produced by strong optical absorption. Therefore, any theory that includes such absorption and has the correct nuclear size will reproduce the overall features of the angular distributions. However, detailed agreement requires a correct treatment of pion-nucleus interaction dynamics.

An accurate theoretical description of elastic scattering data is the first step in the investigation of pion-nucleus interaction. This has been pursued in great detail by using either the multiple scattering formulation or the Δ-hole model. Within the multiple scattering formulation, the main focus is to understand the experimental data in terms of the optical potential, U_{00}, defined by the scattering equation (Equation 12). The analyses based on the Δ-hole model are aimed mainly at a microscopic understanding of the Δ propagation in a nuclear medium. The results from these two approaches are complementary, as we describe below.

Within the multiple scattering formulation, most of the studies of pion-nucleus elastic scattering are based on the FSA optical potential defined by Equation 10. Although this potential is obtained by making several approximations from the exact multiple scattering formulation, it has the nice feature that the pion-nucleus potential is related very simply to the nuclear density $\rho(\vec{r})$ by

$$U_{00}^{\mathrm{FSA}}(\vec{k}', \vec{k}; E) = \langle \vec{k}', \vec{p}_0 - \vec{q} | t(\omega_0) | \vec{k}, \vec{p}_0 \rangle \int e^{-i\vec{q}\cdot\vec{r}} \rho(\vec{r})\, d\vec{r}, \qquad 36.$$

where $\vec{q} = \vec{k}' - \vec{k}$ and the on-shell momentum k_0 is defined by $E = E_A(k_0) + E_\pi(k_0)$ in the pion-nucleus center-of-mass frame. The choices of the momentum $\vec{p}_0$ and πN collision energy ω_0 are model-dependent. The most commonly used "frozen" nucleon model assumes that $\vec{p}_0 = -\vec{k}/A$ and $\omega_0 = E_\pi(k_0) + E_N(k_0/A)$. To use the empirical πN amplitudes to evaluate Equation 36, it is necessary to introduce a procedure to express the πN scattering t-matrix elements defined in the pion-nucleus center-of-mass frame in terms of the matrix elements in the πN center-of-mass frame. Furthermore, the off-shell dependence must be specified. These issues have been investigated in detail, as reviewed in Reference (19). The commonly used computer program PIPIT (22, 27) is based on the FSA optical potential defined in Equation 36. The other widely used optical potential in the code DWPI (23) is based on the coordinate-space representation of the FSA potential (Equation 36). It is essentially a refinement of the Kisslinger potential (20).

By using the nuclear densities constrained by the electron scattering data and reasonable theoretical assumptions, the FSA optical potential (Equation 36) can reproduce the diffractive pattern of the angular distribution in the energy region near the Δ resonance. However, the predicted magnitudes are close to the data only in the forward angles and at $E_\pi \gtrsim 100$ MeV. The results at large angles are rather unsatisfactory, particularly with repect to the positions and depths of the diffractive minima. Typical FSA results at 162 MeV are shown by the dashed curves in Figure 5 for π^- scattering from ^{28}Si, ^{58}Ni, and ^{208}Pb. It was found (53) that the data can be described better by using a density with a radius smaller than what is determined by electron scattering and/or by introducing (54) a shift of collision energy defined by the FSA, namely setting $\omega_0 \rightarrow \omega_0 - \Delta E$ in Equation 36. These phenomenological refinements of the FSA optical potential can lead to better agreement with the data, as shown by the solid curves in Figure 5.

It is important to note here that the good fits to the elastic differential cross sections do not assure that the constructed FSA optical potential in Equation 36

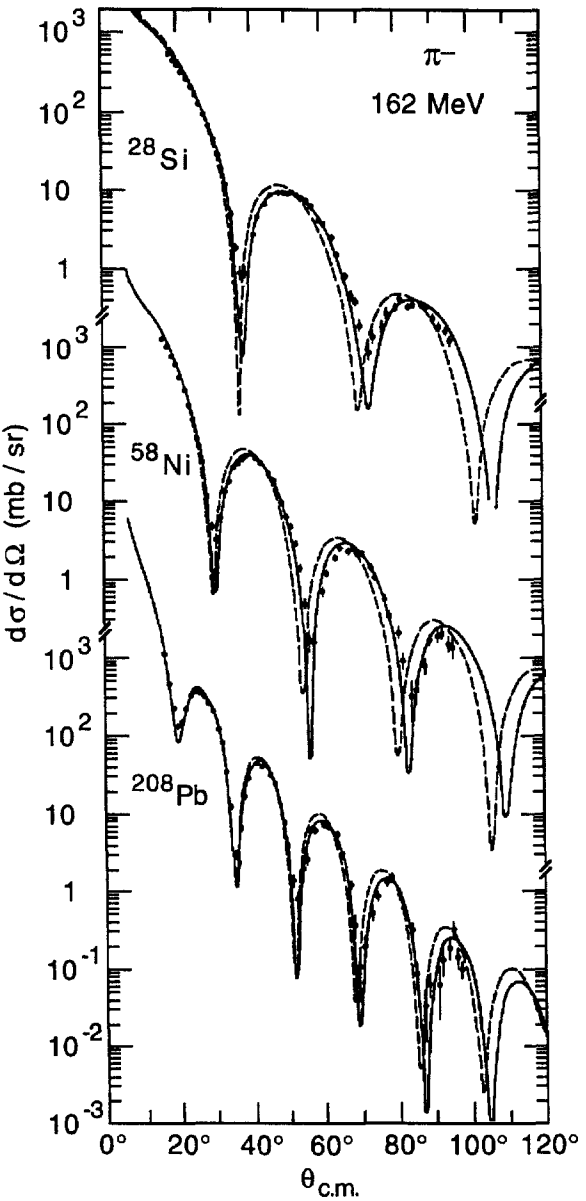

Figure 5 Differential cross sections of π^- elastic scattering from ^{28}Si, ^{58}Ni, and ^{208}Pb. The data are from Reference 53. The dashed curves are from the optical potential calculations of PIPIT (22, 27). The solid curves are obtained (53) from using smaller radii for nuclear density distributions and including an energy shift in evaluating the πN scattering amplitude.

has the correct dynamical content. In general, the predicted total cross sections do not agree well with the data. Nevertheless, the good fits to the elastic differential cross section imply that the resulting pion wavefunctions are reasonably accurate in the region near the nuclear surface. Thus, these semi-phenomenological optical potentials can be used to investigate reactions involving mainly the nucleons near the nuclear surface. This is the case for most of the reactions in the Δ region. Hence, the codes PIPIT and DWPI have been used rather successfully in many distorted-wave calculations of inelastic scattering and charge-exchange reactions.

At low pion kinetic energies of $E_\pi \lesssim 100$ MeV, the differential cross sections predicted by the FSA optical potential U_{00}^{FSA} are typically a factor of 2 to 5 too large in forward angles. It is found that such a large discrepancy cannot be resolved (25, 26, 28) by using the first-order optical potential defined by Equation 8, which is more difficult to evaluate than the FSA optical potential of Equation 36. It is necessary to evaluate (30–32) the second-order optical potential defined by Equation 6 and include the effects due to pion absorption. The calculations of these two effects are, however, very complex and not conclusive, mainly because there is no quantitative understanding of two-nucleon correlations and pion absorption mechanisms. Consequently, it is necessary to develop semi-theoretical optical potentials. The essential idea is to calculate the first-order optical potential in terms of elementary πN amplitudes and nuclear densities as accurately as possible; then the higher-order terms are simply treated phenomenologically. This was pursued (29, 31, 32) by using the form of Equation 13. The phenomenological ρ^2 term is determined by fitting both the elastic scattering differential cross section data and total cross section data. Figure 6 shows the results from Reference (32). Clearly, the ρ^2 term is instrumental in reproducing both the data of the elastic differential cross section (left side) and total cross sections (right side). Similarly, good fits to low-energy data can also be obtained with the widely used MSU optical potential (34), which uses a more sophisticated parameterization of density dependence. The details of the MSU optical potential are summarized in References (36) and (18).

Within the Δ-hole model, pion-nucleus elastic scattering has been studied (79–82) by using Equations 24–31. Alternatively, one can use the optical potential defined by Equations 32–35. As discussed in Section 2.2, the only phenomenological quantity in the Δ-hole model is the spreading potential W_{sp} in Equation 27, which accounts for the $\Delta(\pi)$ absorption. The data can be described by using the following parameterization:

$$W_{\mathrm{sp}} = V_c \rho(r) + V_{LS} \vec{L}_\Delta \cdot \vec{\Sigma}_\Delta f(r), \qquad 37.$$

where $\rho(r)$ is the nuclear density. The second term is the Δ spin-orbit interaction. By fitting both the elastic differential cross sections and the total cross sections, the strengths V_c and V_{LS} are determined. Figure 7 shows the resulting V_c for scattering from ^{4}He (squares), ^{12}C, ^{16}O (circles), and ^{40}Ca (triangles). We see that the imaginary part of V_c, which measures the Δ absorption by the nuclear medium, increases very significantly from $\sim$40 MeV for light nuclei to $\sim$60 MeV for ^{40}Ca. The spin-orbit term is crucial in reproducing the angular distributions, as illustrated

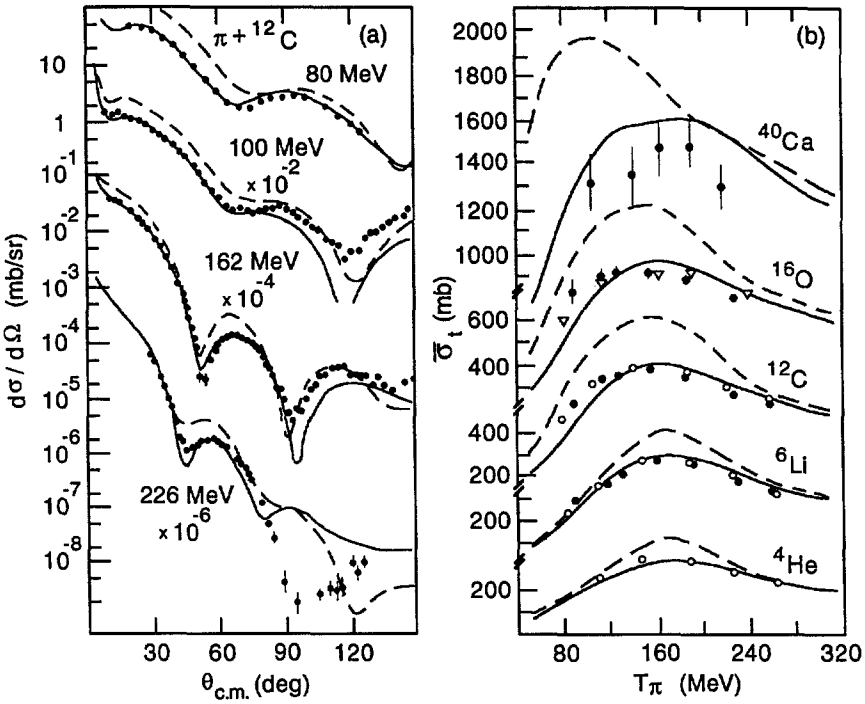

Figure 6 Elastic differential cross sections (left panel) and total cross sections (right panel) for π^+ ^{12}C interactions. The results of Reference 32 are compared with the data from References 41, 64, and 66 (left panel) and from References 39 and 180 (right panel). The dashed curves represent results from using the first-order optical potential. The solid curves are obtained when a phenomenological ρ^2 term is included in the fits to the data.

in Figure 8. Indeed, the rather smooth energy dependence of V_c shown in Figure 7 is possible only when the spin-orbital term is included in the fits.

An important finding from the Δ-hole calculations is that for each Δ-nucleus eigenstate with a definite angular momentum, the cross section in that partial wave is dominated by one or two resonant states, which are coherent sums of Δ particle-nucleon hole components. This collective phenomenon is very similar to the giant dipole resonance due to coherent one-particle–one-hole ($1p$-$1h$) excitations. This is the dynamical reason (12, 79) why the Δ-hole model can be successful in describing the data.

There have been some attempts to understand the dynamical content of the spreading potential. In Reference (83), it was found that the strengths of the phenomenological spreading potential can be understood to a large extent in terms of the $N\Delta$ G-matrix calculated from a many-body Hamiltonian with π and Δ degrees of freedom (84). In the Δ-hole model of Reference (13), the spreading

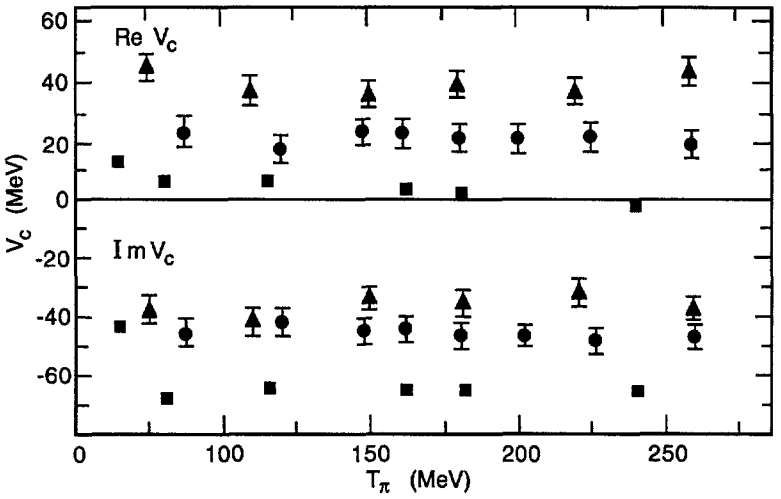

Figure 7 The strength V_c of the spreading potential (Equation 37) of the Δ-hole model. The results are from the compilation of Reference 82. The triangles, circles, and squares denote the results from the fit to the data of pion elastic scattering from ^{4}He, ^{12}C and ^{16}O, and ^{40}Ca, respectively.

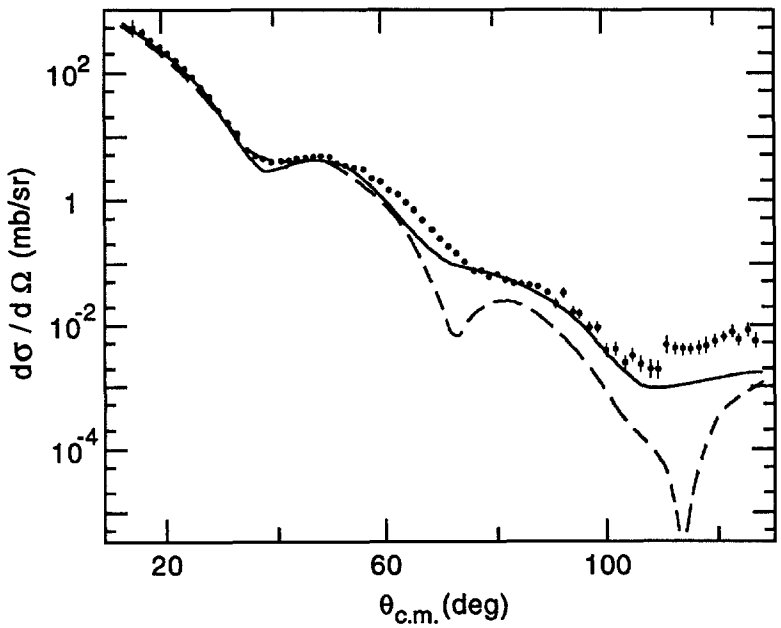

Figure 8 The π^+ ^{16}O elastic scattering cross section at 240 MeV. The curves are from the Δ-hole model calculation of Reference 80. The data are from Reference 43. The dashed curve is obtained when the spin-orbit part of the spreading potential (Equation 37) is not included in the fit to the data.

potential is calculated perturbatively from the effective Lagrangians with parameters constrained by the total cross section data of $\pi^+ d \rightarrow pp$ reactions.

4. INELASTIC SCATTERING

As an isovector particle, the pion can induce three different inelastic scattering reactions from nuclei: charge-conserving ($\pi^{\pm}, \pi^{\pm\prime}$), single charge exchange (SCE) ($\pi^{\pm}, \pi^0$), and double charge exchange (DCE) ($\pi^{\pm}, \pi^{\mp}$). The investigation of these inelastic scattering processes has two objectives. The first is to understand the global features of pion-nucleus scattering mechanisms. This is achieved by performing inclusive (π, π') and ($\pi, \pi' N$) experiments in which the final nuclear states are not identified. The second is to use the characteristics of the pion to probe the structure of nuclei. This is achieved mainly by considering excitations to discrete nuclear states. We discuss these two advances in the next two subsections.

4.1. Inclusive Processes

Fairly extensive data of inclusive ($\pi^{\pm}, \pi^{\pm\prime}$) scattering from nuclei have been obtained at meson factories (37, 85–96). Figure 9 shows typical pion spectra from ($\pi^+, \pi^{+\prime}$) scattering from a wide range of nuclei (88). Each pion spectrum has a quasi-free peak with a width due to nucleon Fermi motion. This suggests that the inelastic scattering is dominated by the knockout of a nucleon to continuum states. However, the medium effects are significant. There are significant shifts of the peak positions from those expected from free πN scattering (marked by arrows in Figure 9). The large medium effects are also reflected in the determined A-dependence $\propto A^{0.4-0.5}$ (see Figure 3), which is weaker than the $A^{0.67}$ of the surface reactions. Thus, simple single scattering calculations using the free πN cross sections as input can give only a very qualitative description of the data. Pion absorption as well as multiple scattering must be accounted for in rigorous theoretical calculations.

The Δ-hole model has been applied (97) to investigate the inclusive scattering from ^{16}O at 162 MeV. The calculation was done by using the DWIA formulation (Equation 16) with $t(\omega)$ replaced by $\tau(E)$ calculated from Equations 33–35 and pion wavefunctions $\chi^{(\pm)}$ generated from the Δ-hole model. It was found that in the Δ peak region, both the spectra and angular distributions of the outgoing pions can be described reasonably well. The results are represented by the solid curves in Figure 10. The agreement is excellent at large angles. At forward angles, the predicted strength is lower than the data at low pion momentum, indicating the importance of nucleon knockout processes that are not included in the Δ-hole model. In the same figure, the dashed curves are from calculations with the medium effects on the Δ neglected. We see that the medium effects, which are mainly due to Pauli blocking and competing absorption channels, are crucial in understanding the data at all angles.

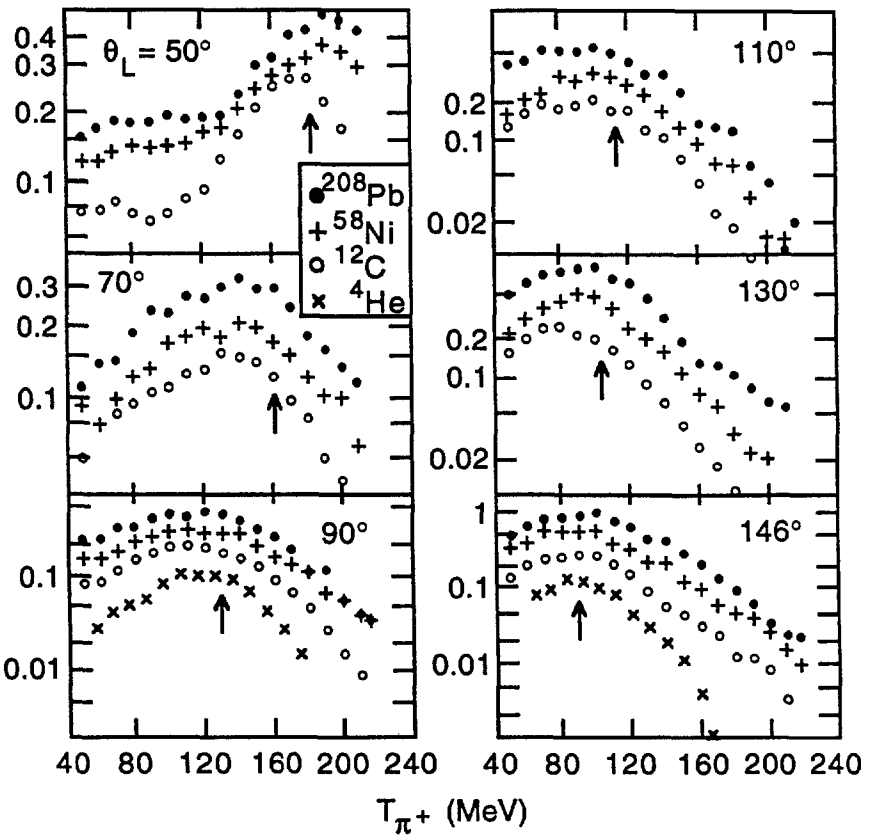

Figure 9 Pion spectra from inclusive (π, π') scattering on various nuclei for various laboratory angles (θ_L) of the outgoing pion, as functions of the outgoing pion's kinetic energy (T_{π^+}). The data are from Reference 88. The arrows indicate the quasi-free peaks expected from assuming that there is no medium effect on πN scattering amplitudes.

Deeper insights into the scattering mechanisms have been obtained from analyzing inclusive $(\pi^{\pm}, \pi^{\pm\prime})$ scattering from ^{3}He and ^{4}He (37, 93–96). The simplicity of these few-nucleon systems allows detailed theoretical calculations of quasi-free mechanisms. In particular, at 180 MeV, where the πN scattering is almost completely determined by the $I = 3/2$ Δ channel, the ratio $^3\text{He}(\pi^+, \pi^+)/$ $^3\text{He}(\pi^-, \pi^-) = 1.73$ is expected from the isospin factors and the numbers of neutrons and protons in ^{3}He. This ratio is indeed observed at the quasi-free peaks. But it quickly deviates from this prediction in the regions away from the quasi-free peaks. The deviation can be qualitatively understood if one assumes that the scattering pions can be more easily absorbed by a *np* pair than by a *pp* pair. This is consistent with the data from pion absorption reactions (see Section 5). By using the

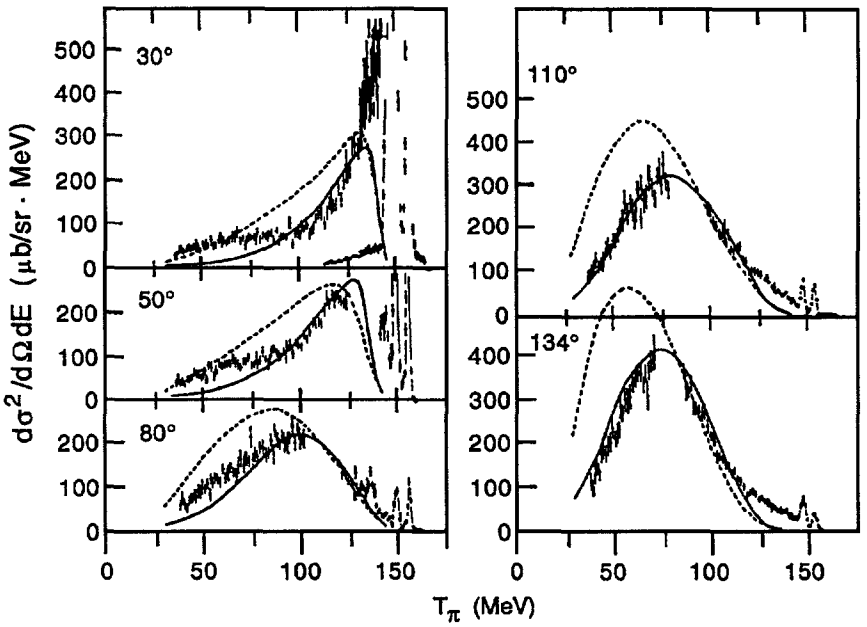

Figure 10 Pion spectra (91) from inclusive $^{16}O(\pi, \pi')$ scattering are compared with the Δ-hole model calculation (solid curves) of Reference 97. The dashed curves are obtained when the medium effects on Δ propagation are neglected.

information provided by DCE data of $He(\pi^-, \pi^+)$, it was also confirmed that the low-energy part of the pion spectrum at forward angles is indeed mainly from double scattering mechanisms; i.e., the $(\pi^\pm, \pi^{\pm\prime})$ cross section differs from DCE cross sections by an isospin factor calculated from assuming $I = 3/2\,\pi N$ scattering. The data of $(\pi^\pm, \pi^{\pm\prime})$ from ^3He and ^4He can be described to a large extent by the DWIA calculations (98) using free πN amplitudes. Clearly, the medium effect on πN scattering is much weaker for A = 3, 4 light nuclei.

The dominance of the quasi-free mechanism is further verified by investigating (99–104) inclusive $(\pi^\pm, \pi^0)$ SCE scattering. Taking into account the isospin factors, most of these data are found to be similar to the inclusive $(\pi^\pm, \pi^{\pm\prime})$ data discussed above. The isospin dependence of the competing pion absorption channels is essential in understanding some crucial differences between the $(\pi^\pm, \pi^{\pm\prime})$ and SCE $(\pi^\pm, \pi^0)$ data.

To further clarify the inelastic scattering mechanisms, experiments on $(\pi, \pi' N)$ were also performed (105–108). The observed ratios between $(\pi^+, \pi^+ p)$, $(\pi^-, \pi^- p)$, and $(\pi^+, \pi^0 p)$ scattering at large angles are rather close to the values of free πN scattering. This further suggests that this reaction is dominated by a quasi-free scattering mechanism. It is also found that the (π, π') cross sections obtained from integrating the $(\pi, \pi' N)$ data are close to those of the inclusive

(π, π') measurements only in the region near the quasi-free peaks. This clearly indicates that the multinucleon removal mechanisms are responsible for the main descrepancy between the Δ-hole DWIA calculations and the data in Figure 10.

The Δ-hole model calculations (109) of $(\pi, \pi' N)$ are much less successful. In particular, the calculations underestimate the magnitude of $^{16}O(\pi^+, \pi^0 p)$ by about 30–55%. It has been suggested (109) that the discrepancy can be removed if additional mechanisms due to $N\Delta$ interactions are included. No substantial calculations have been done to verify this.

Experimental efforts have yielded the A-dependence and energy dependence of the total inelastic scattering cross sections. Both charge-conserving $(\pi^{\pm}, \pi^{\pm\prime})$ and SCE $(\pi^{\pm}, \pi^0)$ scattering behave similarly, as seen in Figures 2 and 3.

The scattering mechanisms have also been studied by investigating (96, 110–113) the inclusive DCE scattering. Both the energy dependence and A-dependence of DCE cross sections have been measured. It was found that the dominant DCE mechanism is sequential SCE from two nucleons in nuclei. This is most clearly seen from the data on few-nucleon systems. Figure 11 shows that the data (96) of $^3He(\pi^-, \pi^+)$ can be described qualitatively by a double scattering calculation. In particular, the double hump structure at forward angles is due to the characteristics of SCE amplitudes. However, the magnitudes at large angles are overpredicted, mainly because of the lack of a proper treatment of the pion distortion. The importance of pion distortion is evident from comparing the $^3He(\pi^-, \pi^+)$ and

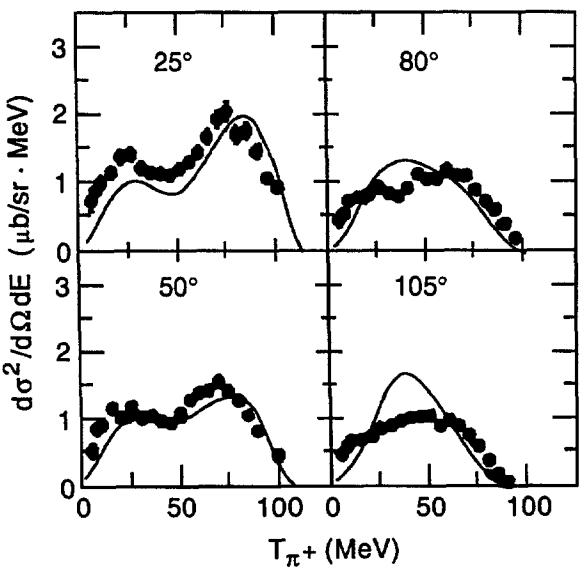

Figure 11 Double scattering calculations of the $^3He(\pi^-, \pi^+)$ reaction are compared with the data. Both the data and calculations are from Reference 96.

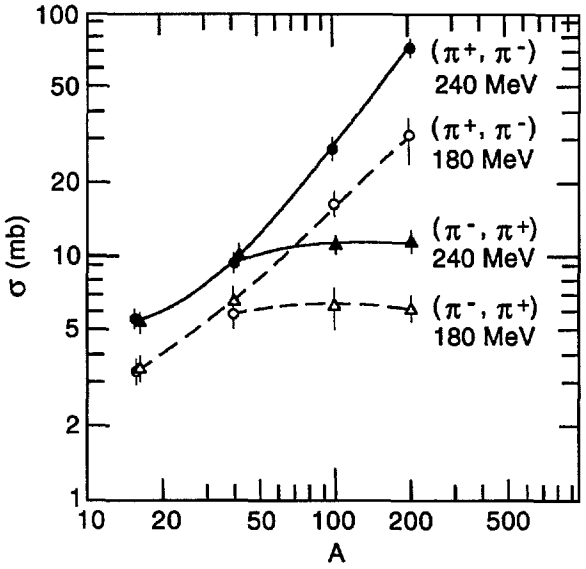

Figure 12 The nuclear mass dependence (A-dependence) of pion double-charge-exchange reactions. The data are from Reference 113. The curves are only to guide the eye.

^{4}He(π^-, π^+) cross sections. It was found that the DCE cross section for ^{3}He is larger than that for ^{4}He. The difference is due to the fact that the distortion in ^{4}He is much larger because there are more *np* pairs to remove the pion flux through absorption.

The double scattering mechanism also appears to be the dominant mechanism for inclusive DCE on heavy nuclei. It was found (112, 113) that the (π^+, π^-) cross section increases with the mass number A, whereas (π^-, π^+) cross sections become saturated at $A \sim 40$ (see Figure 12). The saturation has been interpreted as the result of the competition between the inelastic $(\pi^\pm, \pi^{\pm\prime})$ processes and DCE processes. The measured cross section is described reasonably well by the following expression:

$$\sigma \propto A^{2/3} \frac{Q}{A-Q} \frac{Q-1}{A-1}, \tag{38.}$$

where $Q = N$ for (π^+, π^-) and $Q = Z$ for (π^-, π^+). The factor $A^{2/3}$ characterizes the strong absorption of the incident pions. The other two factors reflect the probability for the SCE to take place on the first and second nucleons. Additional evidence of the dominance of the double scattering mechanism is that (110, 113) the angular distributions of DCE on heavy nuclei are consistent with those of four-body (πNNA_{A-2}) final states.

The theoretical calculations (14, 114) for inclusive DCE reactions are all based on semiclassical approximations for pion propagation. The calculated energy

dependence of the total DCE cross section fails to reproduce the data. The predicted angular distributions are in poor agreement with the data. This is not surprising, since the DCE reactions are sensitive not only to pion distortion but also to two-nucleon correlations. Accurate two-nucleon correlations were not available to those earlier calculations.

4.2. Excitation of Discrete States

One of the objectives of building meson factories was to use pions as probes of the structure of nuclei. This was realized rather successfully in the study of inelastic scattering $(\pi^{\pm}, \pi^{\pm\prime})$ leading to discrete final nuclear states.

Most of the theoretical investigations are carried out by using the DWIA model defined in Equation 14. The pion wavefunctions are generated from an optical potential that accurately reproduces the elastic scattering differential cross section data. Such optical potentials can be obtained by adjusting the parameters of U_{00}^{FSA} defined by Equation 10 or the model in Equation 13, including the ρ^2 term.

It was established (115–117) in the early 1970s that the FSA-DWIA approach is reliable only in cases where the pion inelastic scattering is dominated by the excitation of nucleons near the nuclear surface, where the average nucleon momenta are low and the medium modifications of the πN interactions are weak. Therefore, the FSA-DWIA model succeeds mainly in the energy region near the Δ excitation, where the strongly absorptive nature of the pion-nucleus interaction suppresses the pion wavefunctions in the nuclear interior. This also means that the FSA-DWIA approach can be used to meaningfully explore the nuclear structure only in cases where the transition densities are peaked near the nuclear surface.

The main advantage of using pions to probe nuclear structure is that the elementary πN amplitude has a strong isospin dependence. This interesting feature is also most useful in the Δ region ($E_\pi \sim 160$ MeV) where the πN interaction is dominated by the P_{33} partial wave. Because $t_{\pi^+ p} \sim 3t_{\pi^+ n}$ and $t_{\pi^- n} \sim 3t_{\pi^- p}$ in the P_{33} channel, we have within the FSA-DWIA approach the following interesting relation:

$$\frac{\sigma_{\pi^+}}{\sigma_{\pi^-}} \sim \left| \frac{3M_p + M_N}{M_p + 3M_N} \right|^2, \qquad 39.$$

where the nuclear transition amplitudes M_p and M_n are proportional to the proton and neutron transition densities, respectively. Equation 39 indicates that the relative importance of the neutron and proton excitations can be revealed by comparing the π^+ and π^- data in the Δ energy region. For a pure proton (neutron) excitation, one would see a striking ratio, $\sigma_{\pi^+}/\sigma_{\pi^-} \sim 9(\frac{1}{9})$. Investigations in this direction have been pursued (45, 47, 52, 53, 56, 69, 118–128).

Figure 13 shows an interesting result from a very thorough investigation (124, 125) of the structure of ^{13}C. Nuclear transitions are calculated from well-established shell models (129, 130). The predicted results for the excited states $^{13}\mathrm{C}(\frac{9}{2}^+, 9.5$ MeV) and $^{13}\mathrm{C}(\frac{9}{2}^+, 16.05$ MeV) are in very good agreement with the data in both shape and magnitude. This result clearly verifies the shell-model predictions that

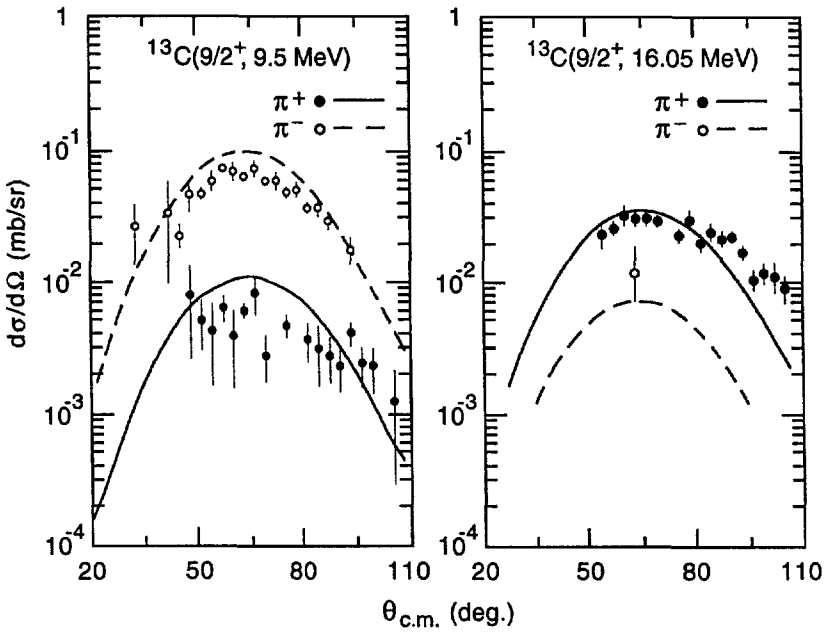

Figure 13 The DWIA calculations (121) of $^{13}C(\pi^{\pm}, \pi^{\pm\prime})$ leading to the excited states $^{13}C(\frac{9}{2}^+, 9.5\ \text{MeV})$ and $^{13}C(\frac{9}{2}^+, 16.05\ \text{MeV})$ compared with the data (125).

the $(\frac{9}{2}^+, 9.5\ \text{MeV})$ state is reached mainly by the neutron excitation and the $(\frac{9}{2}^+, 16.05\ \text{MeV})$ state mainly by the proton excitation. These results also strongly support the interpretation that the $(\frac{9}{2}^+, 9.5\ \text{MeV})$ state consists of a $d_{5/2}$ neutron coupled to the $^{12}C(2^+, 4.44\ \text{MeV})$ state.

Another interesting advance is to use Equation 39 to extract the relative strength between the neutron and proton excitations. Figure 14 shows the transition amplitudes extracted (69) from the data of inelastic scattering of π^+ and π^- from the $N = 27$ nuclei ^{48,50}Ti, ^{52}Cr, and ^{54,56}Fe. The data clearly indicate that the usual collective model with density scaled by (N/Z) is ruled out by the pion data.

Within the multiple scattering theory, it is important to ask whether multistep transitions are important in inelastic scattering. It was found (76, 131, 132) that in the Δ region, the multistep transition effects are negligibly small for strongly excited states. On the other hand, some multistep transitions have some cancellations and lead to very different predictions (76). This, however, has not been pursued experimentally.

From the point of view of the Δ-hole model, the FSA-DWIA approach is not justified because the medium-corrected τ defined by Equations 33–35 is clearly different from the free πN t-matrix. This was explored in detail in References (133) and (134). Within their model, it was found that the medium effects

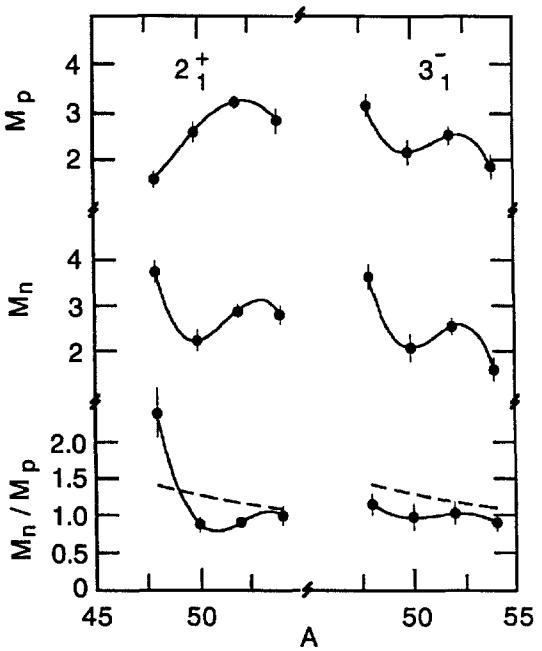

Figure 14 The nuclear mass dependence (A-dependence) of the proton (neutron) excitation amplitudes $M_p(M_n)$ extracted from pion inelastic scattering from $N = 28$ nuclei ^{48}Ca, ^{50}Ti, ^{52}Cr, and ^{54}Fe (69). The results on the left-hand side (right-hand side) correspond to the first 2^+ (3^+) final nuclear states. The solid curves are only to guide the eye. The dashed curves are the predictions of the usual collective model with densities scaled by the N/Z ratio.

indeed are significant. This is illustrated in Figure 15 for $(\pi^-, \pi^{-\prime})$ from ^{12}C. However, it is important to note that the differences between the solid and dashed curves in Figure 15 do not reflect the accuracy of the usual FSA-DWIA approach, since in this FSA calculation the elastic scattering data are not reproduced accurately. The discrepancies between the FSA-DWIA results (dashed curves) and the data can be largely removed if one uses the pion wavefunctions generated from an optical potential that accurately fits the elastic scattering data. The success of the commonly used FSA-DWIA approach is due to the strongly absorptive nature of the pion-nucleus interactions, as discussed above and, for example, in Reference (117).

On the other hand, medium effects can induce excitations that are absent from the FSA-DWIA approach. This is perhaps the main reason why some weakly excited states, which are predicted by well-established shell models, are poorly described by the FSA-DWIA calculations. One example is the ratio $\sigma(I = 1)/\sigma(I = 0)$ between the two 1^+ excitations in ^{12}C. In the FSA-DWIA approach, this ratio is 2 as constrained by isospin conservation. The experimental value (126) is

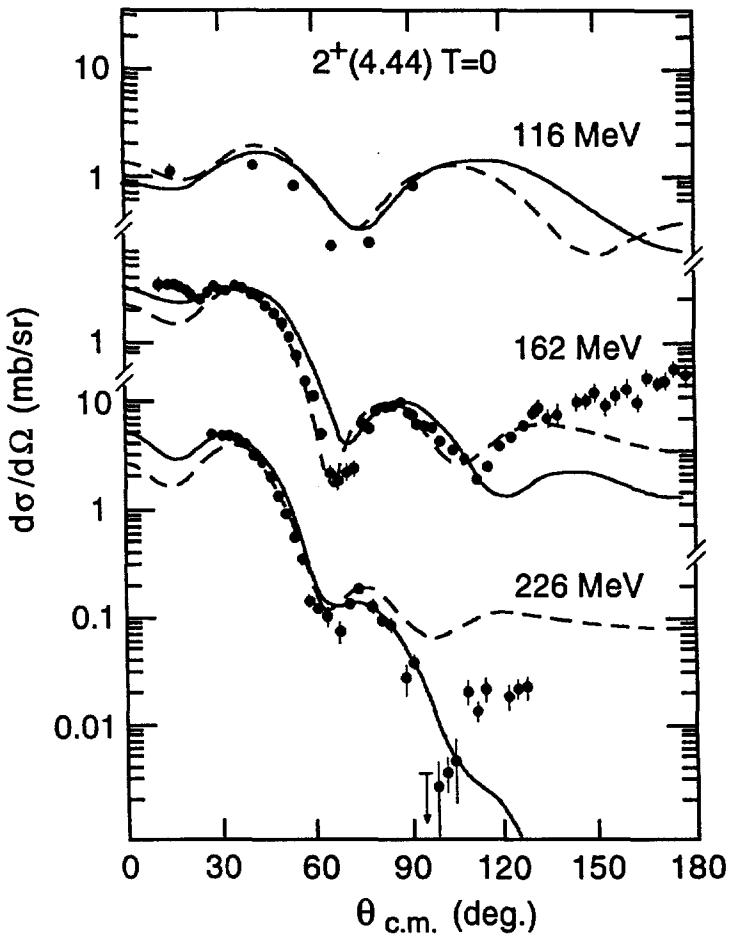

Figure 15 Δ-hole calculations (133) of $^{12}C(\pi, \pi')^{12}C^*$ inelastic scattering compared with the data (37). The dashed curves are obtained when the medium effects on the Δ propagation are neglected.

only about 1.2. Including an $N\Delta$ interaction in the Δ-hole model is a possible way to understand these data (135). Unfortunately, the DWIA based on the Δ-hole model has not been fully exploited to investigate various nuclear structure problems in conjunction with the most sophisticated nuclear models. Furthermore, the Δ-hole calculations for inelastic scattering become technically very complex for non-closed-shell nuclei (136) and for large-A systems. Nevertheless, the results from the Δ-hole model have provided important information to assess and/or understand both the successes and the limitations of the extensively employed FSA-DWIA approach.

Thanks to its isovector nature, the pion can serve as a probe to study the isospin structure of nuclear excitations, which may be difficult if not impossible to study otherwise. This has motivated extensive measurements of exclusive single-charge-exchange (SCE) (137–141) and double-charge-exchange (DCE) (142–152) reactions. The DCE is most interesting, since at least two nucleons must be involved in nuclear transitions and thus one can hope to learn about short-range correlations from this reaction.

The most-studied exclusive charge-exchange reactions are those leading to the isobaric analog states, which can be reached from the target ground states by changing only the nucleon's charge without altering its spatial distribution. The simplest theoretical approach (153, 154) for investigating this "elastic" charge-exchange scattering thus is based on an extension of the elastic FSA first-order pion-nucleus potential to account for the isospin dependence as induced by the elementary πN t-matrix. It turns out that this simple approach, using either DWIA or coupled-channel calculations, is not successful in describing charge-exchange reactions leading to analog states. Including a second-order potential evaluated using closure and FSA in the calculations does improve the agreement with the data, but large discrepancies remain. For example, the SCE calculations of References (121) and (154–158) all underestimate the $^{13}C(\pi^+, \pi^0)$ data in the Δ region by a factor of two or more at the forward angles and do not reproduce the position of the first diffractive minimum. The corrections to FSA, such as binding and Pauli effects, significantly improve the agreement with the data (159). The Δ-hole calculations (136, 160–162) give a better description of these data, although significant discrepancies remain. Higher-order effects, such as the coupling with other excited states, have been investigated (163–165), but no solution to the problem has been found. It appears that the SCE reactions leading to analog states involve the nucleon distribution in the whole volume of nuclei and hence are more sensitive to pion wavefunctions. Therefore, the difficulty could originate from using an inaccurate description of pion absorption effects, which can strongly influence the pion wavefunctions in the interior of the nucleus where the analog transitions also take place. The situation is very similar to the failure of FSA-DWIA models in describing inelastic scattering involving excitations that are not surface peaked.

For DCE leading to analog states, the simplest approach is to assume sequential SCE with intermediate states restricted to analog states and transitions defined by the FSA first-order potential (Equation 10). The results from such an approach (153, 164, 166) disagree severely with the data in most cases, even if nucleon-nucleon correlations are included through a second-order potential (Equation 18). This shows that DCE reactions involve transitions to non-analog intermediate states. For example, we must observe that ratio $R = \frac{^{16}O(\pi^+,\pi^-)^{16}Ne}{^{18}O(\pi^+,\pi^-)^{18}Ne} \sim 0$ if only the analog transition is allowed. The experimental value is $R \sim 1/3$, which can be understood (167, 168) only when the non-analog transitions due to the core polarization of ^{16}O are accounted for appropriately. Similar calculations (169) for heavy nuclei have found the same large effects due to non-analog transitions.

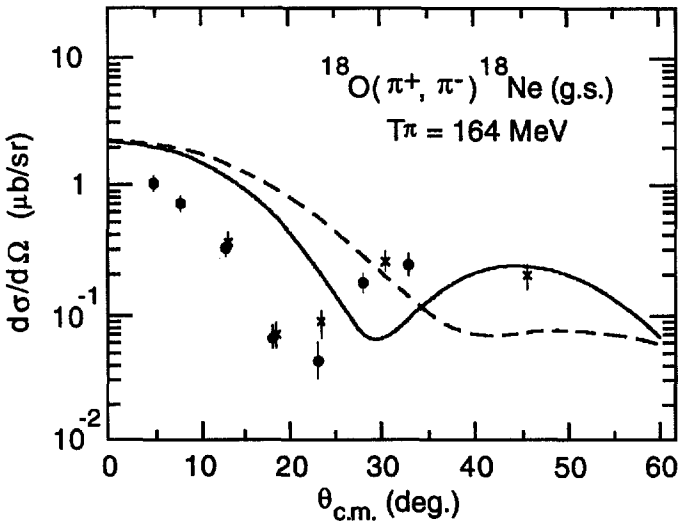

Figure 16 Δ-hole calculations (170) of pion double-charge-exchange scattering from ^{18}O compared with the data (142, 143). The dashed curve is obtained when the non-analog intermediate states are neglected in the calculations.

Subsequent theoretical calculations have further established this. Figure 16 shows the results from Δ-hole calculations (170) for $^{18}O(\pi^+, \pi^-)^{18}Ne$(g.s.). We see that the difference between the solid curve and the dashed curve is due to transitions through non-analog intermediate states. The disagreement with the data is still very significant, indicating that more corrections are needed. Similar difficulties are also found in all FSA-DWIA calculations (168). As in the case of SCE, the failure here of all theoretical models is mainly due to an inaccurate description of pion absorption effects on pion wavefunctions inside nuclei. Other mechanisms, such as that due to six-quark formation (172, 173) or rescattering from virtual pions in nuclei (174, 175), could also be possible. However, these investigations of "exotic" mechanisms are not conclusive, mainly because the basic nucleon-nucleon correlations used in the calculations are not under control. Glauber multiple scattering calculations (176–179) have also been performed for DCE reactions, although the applicability of such an approach is questionable in this energy region.

Apart from analog states, charge-exchange reactions have also been used to explore other new aspects of nuclear structure. For example, SCE has revealed (139, 140) isovector $I = 1$ giant resonances that are not well investigated using other probes. Such a resonance state is especially interesting because it can be described as a breathing mode, wherein the proton and neutron distributions have oscillating radii 180° out of phase.

5. ABSORPTION REACTIONS

The absorption of pions by nuclei has long been of interest to nuclear physicists. In contrast to more common probes of nuclei, such as protons and electrons, the pion is a boson and thus can be absorbed. However, the pion cannot be absorbed on a free nucleon and still conserve energy and momentum. Therefore, at least two nucleons must be involved in the absorption process. This is largely true even for nucleons inside a complex nucleus, since the single-particle momentum that must be provided by the nucleus to make pion absorption on a nucleon in the nucleus obey energy and momentum conservation is well above the Fermi momentum.

These kinematic considerations led researchers long ago to suggest that pion absorption would be an excellent tool for the study of two-nucleon correlations in nuclei, and in fact much of the justification for the three meson factories had to do with the anticipated use of pions as such tools. As discussed below, pion absorption turned out to be considerably more complicated than just two-nucleon absorption and has become a field of study in its own right. As an example of an early indication of the interesting aspects of pion absorption, Figure 2 shows the results of an experiment (180) that separated the various reaction channels that make up the total cross section for pion-nucleus interactions on carbon. It is apparent that the effect of the Δ resonance is most prominent in the absorption channel. We still do not have a good understanding of this observation, although it is clearly significant for the study of pion-nucleus interactions.

Several early experiments indicated that pion absorption in nuclei in the region of the Δ resonance often involved more than two nucleons. McKeown et al. (86) measured $(\pi^{\pm}, p)$ reactions on a variety of nuclear targets and analyzed the data to determine the average number of nucleons involved in absorbing the energy and momentum of the incident pion. The analysis had significant systematic uncertainties and became somewhat controversial, but it indicated that the average number of participating nucleons could be as high as six for a heavy nucleus. Other experiments (181–194) used the angular and energy correlations between the outgoing nucleons in (π, NN) reactions to isolate the part of the absorption cross section that involved only a neutron-proton pair. It was found that a major part of the absorption cross section, more than half for heavy nuclei, involved more than two nucleons in a significant way. This part of the absorption cross section became known as multinucleon absorption.

It is important at this point to be careful with terminology so as to avoid confusion and not to obscure the important physics issues. One expects to find initial-state interaction (ISI) effects, such as scattering of the pion before absorption on a pair of nucleons, and final-state interaction (FSI) effects, such as scattering of the outgoing two nucleons on other nucleons in the nucleus. These ISI and FSI effects would contribute to making the average number of nucleons participating in the process greater than two, even if the primary absorption process is two-nucleon absorption. This would not involve new physics, although the details of

the absorption process would still be of interest. However, if there were a coherent process involving more than two nucleons, then we might indeed learn something important about the interactions of hadrons at short distances.

The distinction between a process that entails sequential classical scatterings in the nucleus and one that entails a coherent interaction on several nucleons in the nucleus becomes blurred as the distance between interactions becomes small. The task of the experimenter has been to design measurements that can cleanly access a specific process or processes. In the end, we will understand the absorption process and whether there is really new physics involved only by understanding the complete picture of the interaction.

Whereas most early experiments on pion absorption in nuclei involved medium to heavy nuclei (reviewed in Reference 5), in recent years the concentration has been primarily on light nuclei. Several groups have used few-body nuclei to isolate the various processes in the absorption reaction, and this strategy has paid off in considerable new insight. Another important feature of these later experiments is the use of large solid-angle coverage. The aim is to learn as much as possible about each event and to access all important types of absorption events. Small-solid-angle experiments, especially on light nuclei, can sometimes be kinematically complete, but they may be totally insensitive to some important types of events. We have learned that it is important to have large solid-angle and low energy thresholds in order to measure as much as possible about every event. In the following, we mainly discuss the results from these experiments on light nuclei.

5.1. The Two-Nucleon Absorption Process

The prototype of the two-nucleon absorption (2NA) process is the $\pi^+ d \rightarrow pp$ reaction. This reaction has been much studied both experimentally and theoretically (reviewed in Reference 2). A review of the experimental work (208, 209) contains most of the data taken at the meson factories. Because all particles in the initial and final states are charged, it is possible to study the reaction in both directions. With regard to pion absorption, angular distributions have been measured for a number of energies below and across the Δ resonance.

The total cross section for $\pi^+ d \rightarrow pp$ has been determined precisely in the energy region of $T_\pi < 300$ MeV, where the Δ resonance is a prominent feature. Although the $\pi^+ d \rightarrow pp$ reaction is a prototype of the two-nucleon reaction in nuclei, it does of course address absorption only on a ${}^3S_1 + {}^3D_1$ nucleon pair. The question of whether 2NA in the nucleus is similar to π^+ absorption on a deuteron is indeed an interesting one, and we address this question next.

A number of experiments (197, 198, 200, 207) have demonstrated that 2NA of pions in nuclei is dominated in this energy region by absorption on deuteron-like pairs. These experiments have used the particular properties of ^{3}He to reach this conclusion. The $\pi^+ {}^3$He process of 2NA involves absorption on pn pairs in either an $I = 1$ or $I = 0$ state. In contrast, the $\pi^- {}^3$He 2NA process involves absorption only on an $I = 1$ pp pair. By comparing these two reactions at the same energies, one

can try to separate the $I = 0$ and $I = 1$ 2NA processes. Several groups have done so and found that, in the region of the Δ resonance, $I = 0$ absorption dominates by a factor of about 20. This is understood as a result of the dominance of the Δ resonance, as the intermediate Δ-nucleon s-state, which dominates absorption for an $I = 0$ nucleon pair, is forbidden for absorption on an initial $I = 1$ pair (197).

Therefore, we believe we have a good understanding of 2NA in nuclei in this energy region. It is dominated by absorption on $I = 0$ pn pairs and is sometimes referred to as quasideuteron absorption. Contributions from absorption on $I = 1$ pairs is much less important, especially near the peak of the Δ resonance. These experimental observations can be largely explained by a theoretical calculation (212) based on a many-body Hamiltonian with π and Δ degrees of freedom (84) and the information from the Δ-hole model.

5.2. Absorption on ^{3}He and ^{4}He

Most experiments in recent years have concentrated on the investigation of absorption on light nuclei, especially ^{3}He and ^{4}He. This focus is due to the possibility to perform kinematically complete experiments and the desire to minimize effects of a complicated nuclear environment. Also, for some time it was suspected that a large change occurred in the pion absorption process between ^{3}He and ^{4}He, possibly indicating a major role for absorption on four nucleons or a strong dependence on the internucleon distance.

An example of an early experiment on ^{3}He is that of Backenstoss et al. (182) at PSI. This experiment used fairly small solid-angle detectors to measure correlations of outgoing protons. It was found that, in addition to the expected 2NA contribution, there is a significant contribution from a process that significantly involves all three nucleons. The solid-angle coverage of the early experiments was limited, but with the assumption that the 3NA contribution was described well by phase space in the final state, extrapolations to the unmeasured regions indicated that the 3NA process was comparable to the 2NA process in ^{3}He. The validity of such extrapolations was a major question for later experiments.

The LADS experiment at PSI (196) was designed to cover as much solid angle as possible to provide detailed and complete information on the outgoing particles following pion absorption. Most of the LADS data were taken with ^{3}He and ^{4}He, for the reasons mentioned above, although some data were also taken with heavier nuclei. To summarize the ^{3}He data, LADS confirmed that the 3NA process is indeed a significant part of the total absorption cross section. Signatures of the ISI process are apparent and indicate that, although ISI is present as expected, it explains no more than about half of the 3NA cross section seen (see Figure 17). No indication for FSI is seen, but at these energies FSI is expected in any case to be less important than ISI in ^{3}He because of the different strengths of the πN and NN interactions.

The LADS experiment and other experiments on ^{4}He have concentrated on the relative importance of 2NA, 3NA, and 4NA processes. As discussed above, the large solid-angle coverage and low energy threshold for protons of LADS were

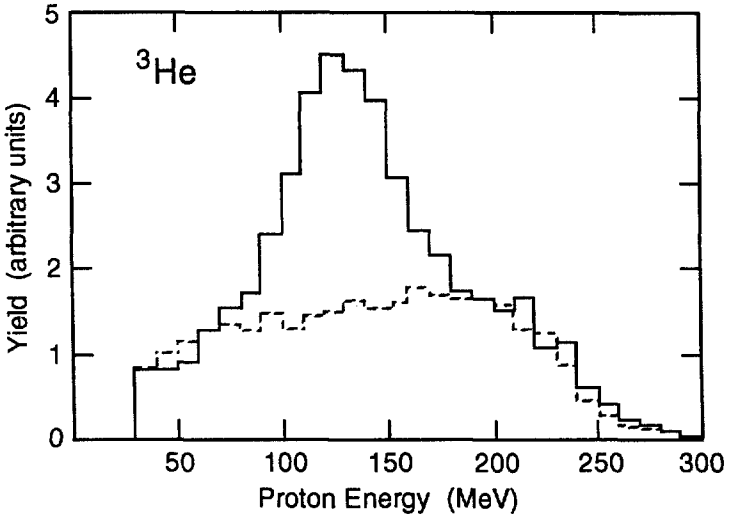

Figure 17 Yield (solid line) of protons for ^{3}He(π^+, *ppp*) events between the polar angles 15° and 25°. The incoming pion kinetic energy is 239 MeV. The dashed line is a phase-space simulation of a three-proton final state, arbitrarily normalized to fit the tails. The data are from Reference 202.

crucial for defining precisely the role of each of these processes. Important results of these ^{4}He experiments include the following:

- The (π^+, *ppp*) reaction appears similar to that on ^{3}He (203). This indicates that a coherent 3NA process may be an important part of the absorption reaction in any nucleus with more than two nucleons. Smaller-solid-angle experiments at TRIUMF (221) have yielded interpretations somewhat at odds with this result. However, the lack of phase space coverage at TRIUMF may be a serious problem for these interpretations.
- There is evidence for multinucleon reactions involving ISI and FSI, but most of the multinucleon absorption process does not appear to involve ISI or FSI.
- As hinted by some early experiments, it appears that the (π^+, *ppn*) cross section is significantly greater than the (π^+, *ppp*) cross section (204) (see Figure 18). This in some ways is a real surprise. If ISI were important at all, one would expect a process in which the π^+ first scattered from a proton and then absorbed on a *pn* pair (thus producing three protons in the final state) to be dominant, simply because of the relative sizes of the π^+p and π^+n scattering cross sections in this energy region. The experiment says the opposite, and this result is not understood at present.
- The (π^+, *pppn*) cross section is weak (204), which provides no support for a postulated Δ-Δ process (213). This postulate can be ruled out as an important player in multinucleon pion absorption.

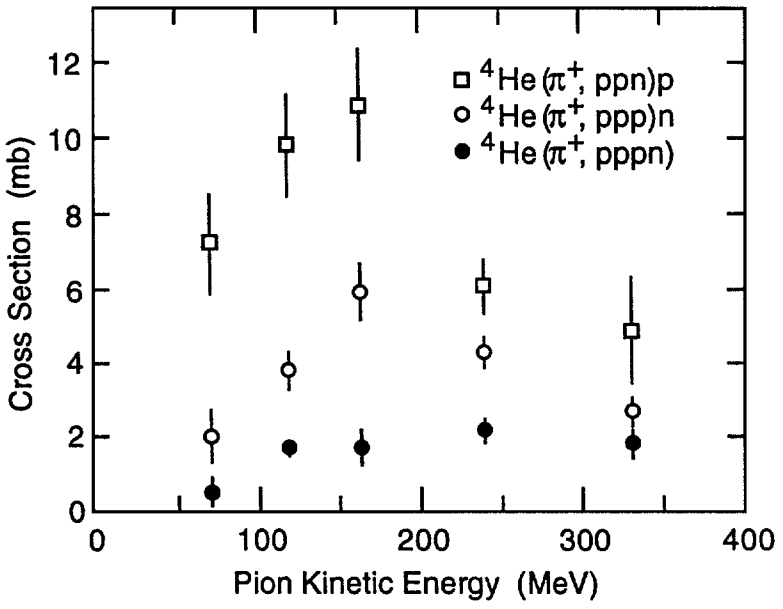

Figure 18 Cross sections for various processes of π^+ absorption on ^{4}He. The data are from Reference 204.

- Recent experiments (205) have also provided precise measurements of the total absorption cross section on ^{4}He. We now have a much better knowledge of the A-dependence of the total absorption cross section in the Δ resonance region, especially for light nuclei. These results are discussed in more detail below.

5.3 Absorption on Nuclei with $A > 4$

This is where the absorption story began, with first indications for an interesting multinucleon process coming from experiments on heavy nuclei. Although most recent work has been on light nuclei, there are some results on heavier targets. Kotlinski et al. (211) see evidence for ISI contributions to 3NA, and the fractional contribution from ISI appears to be fairly constant with A. No explicit signatures for FSI are seen, but this may not be surprising given the subtlety of the signatures.

The BGO Ball experiment at LAMPF (see (222) and references contained therein) has reported interesting results for pion absorption on heavier nuclei. In general they observe significant numbers of nucleons sharing the energy and momentum of the absorbed pion.

Rowntree et al. (210) reported results for absorption on several heavier nuclei. They were able to measure fairly directly the probability that various numbers of

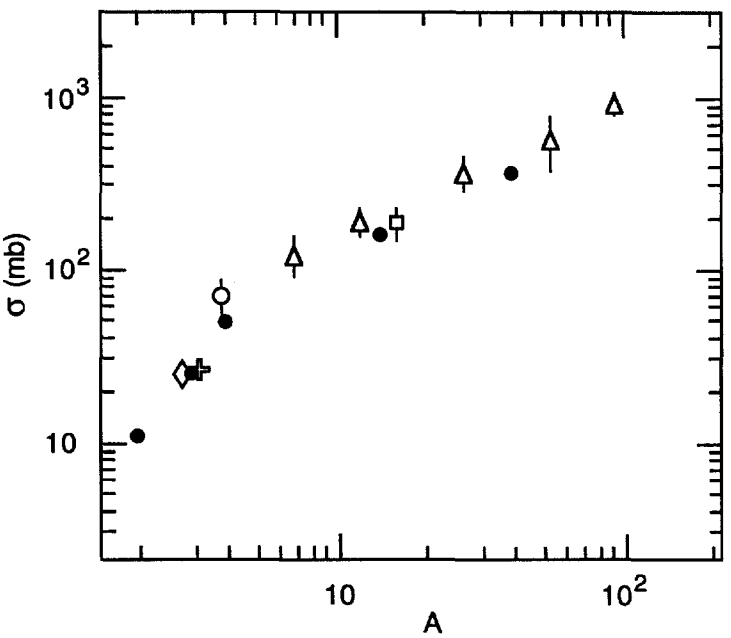

Figure 19 The nuclear mass dependence (A-dependence) of total absorption cross sections at 165 MeV. The data are from References 180, 191, 192, 195, 199, and 201.

nucleons emerge following absorption. These results can be compared to the results of McKeown et al. (86), which were important in raising the original questions about multinucleon absorption. The Rowntree et al. multiplicities are consistent with those reported by McKeown et al. in that the average number of nucleons substantially involved in the absorption process appears to be considerable and at least somewhat A-dependent. The more recent results do indicate a smaller A-dependence than that of Reference (86).

Precise, reliable values for pion total absorption cross sections have been frustratingly difficult to obtain over the years. However, we now have quite a good idea of the A-dependence, as shown in Figure 19. The transition from the deuteron to heavier nuclei, where the A-dependence appears to follow a power law, is reasonably smooth. This is in contrast to indications from earlier data (199), which showed a sudden jump between ^{3}He and ^{4}He. The power law exponent for heavier nuclei is roughly 0.75 (see also Figure 3), which means that absorption is taking a greater and greater share of the geometrical total cross section as a function of mass number A.

Theoretical investigations of pion absorption reactions are not very successful. The contribution of two-body absorption to inclusive (π, p) on a wide range of nuclei has been investigated (212) using a πNN model (84) and the Δ-hole model. The calculated cross sections agree with the data only in the region near quasi-free

peaks. There are also investigations of exclusive (π, NN) (214, 215) reactions leading to discrete nuclear states. There are no satisfactory theoretical explanations of most of these exclusive data, although DWIA calculations (216) of (π, NN) assuming a two-body absorption mechanism reproduce main features of the data for light nuclei.

6. RELATION TO CURRENT RESEARCH

We have reviewed most of the major advances in our understanding of pion-nucleus interactions in the past three decades. Here we discuss how this information is related to several research programs of current interest.

With new electron and photon facilities, such as those at Jefferson Laboratory, MIT-Bates, and Mainz, experiments are exploring the nuclear dynamics originating from fundamental quark-gluon degrees of freedom. The data for such efforts are from experiments that often involve measurements of pion channels, such as $(e, e'\pi)$ and $(e, e'\pi N)$ reactions in the Δ region, but at high momentum transfers. Obviously, genuine new physics, such as Δ components in nuclei (223) and the six-quark dynamics of $N\Delta$ interactions (224), can be identified only when these data are analyzed using theroretical models that are well constrained by the existing data of pion-nucleus interactions. In particular, the strong coupling between the scattering channel and absorption channel must be accounted for correctly. It is highly desirable, and perhaps necessary, to revive and extend the Δ-hole model to analyze these new data. The main challenge here is to perform fully microscopic calculations in which the spreading potential W_{sp} of Equation 27 is also calculated from a theoretical model of pion absorptions on two-nucleon and multinucleon systems. Similar considerations must also be taken to analyze the pion data from neutrino-induced nuclear reactions in the few-GeV region. It has been recognized (225) recently that an accurate account of these data is very important to a correct interpretation of the next-generation neutrino-oscillation experiments to be conducted in the near future.

The investigation of relativistic heavy-ion collisions has become a major research activity, aimed at investigating the phases of matter at high densities and/or high temperatures. In such violent collisions, pions are produced abundantly. Analyses of the data of pions produced in the baryon-rich region are particularly relevant to our understanding of pion-nucleus interactions. Theoretical approaches appropriate for analyzing these data must be consistent with the data on pion-nucleus interactions. For example, an approach should at least reproduce the global features of pion-nucleus cross sections displayed in Figures 1–3. Only approaches that pass such a test should be applied to the much more complex situations in relativistic heavy-ion collisions, such as the propagation of pions in Δ-rich systems. This is an important step to understand reaction mechanisms and to determine whether one has reached the densities at which the quark-gluon plasma can be created. The same considerations must be taken into account when analyzing new pion data from RHIC and eventually from LHC.

In recent years, a great deal of progress has been made in the development of nuclear structure theories. The properties of light nuclei can now be predicted starting from realistic nucleon-nucleon interactions by using the quantum Monte Carlo methods (226). In conjunction with the new opportunities at the anticipated rare-isotope accelerators, theoretical models for stable nuclei have been extended to predict how the nuclear properties change as nuclei acquire more neutrons or protons and move away from the stability line. Pion-nucleus reactions can be very effective in testing these new nuclear theories. For example, the neutron transition densities predicted by quantum Monte Carlo calculations have been found (227) to be consistent with the data of $\mathrm{Li}(\pi, \pi')\mathrm{Li}^*$ in the Δ region, where the strong isospin dependence of the πN interaction, as discussed in Section 4.2, can be used to distinguish between the neutron and proton excitations. It will be interesting to perform the same test on nuclear models that are being used to predict the change of nuclear properties as the N/Z ratio gradually moves off the stability line. More detailed tests of these new nuclear structure theories can be made by using the unique pion DCE and pion absorption reactions. As discussed in Sections 4 and 5, these two reactions involve at least two nucleons and are sensitive to nuclear correlations. Thus, the effort in this direction will be important not only to develop nuclear structure theories but also to resolve many long-standing problems in understanding these two novel reactions in particular and pion-nucleus interactions in general.

ACKNOWLEDGMENT

This work was supported by the U.S. Department of Energy, Nuclear Physics Division, under contract no. W-31-109-ENG-38, and by the U.S. Department of Energy under grant no. DE-FC02-94ER40818.

The *Annual Review of Nuclear and Particle Science* is online at http://nucl.annualreviews.org

LITERATURE CITED

1. Carroll AS, et al. *Phys. Rev. C* 14:635 (1976)
2. Garcilazo H, Mizutani T. *π-NN System.* Singapore: World Sci. (1990)
3. Koltun DS. *Advances in Nuclear Physics*, ed. M Baranger, E Vogt, 3:71 (1969)
4. Hüfner J. *Phys. Rep.* 21:1 (1975)
5. Ashery D, Schiffer JP. *Annu. Rev. Nucl. Part. Sci.* 36:207 (1986)
6. Gibbs WR, Gibson BF. *Annu. Rev. Nucl. Part. Sci.* 37:411 (1987)
7. Weyer H. *Phys. Rep.* 195:295 (1990)
8. Watson KM. *Phys. Rev.* 89:575 (1953); 105:1388 (1957); 30:565 (1958)
9. Kerman A, McManus H, Thaler R. *Ann. Phys.* 8:551 (1959); Feshbach H, Gal A, Hüfner J. *Ann. Phys. (NY)* 66:20 (1971)
10. Kisslinger LS, Wang WL. *Phys. Rev. Lett.* 30:1071 (1973); *Ann. Phys.* 99:374 (1976)
11. Hirata M, Lenz F, Yazaki K. *Ann. Phys.* 108:116 (1977); Hirata M, Koch JH, Lenz F, Moniz EJ. *Ann. Phys.* 120:205 (1979)

12. Klingenbeck K, Dillig M, Huber MG. *Phys. Rev. Lett.* 41:387 (1978)
13. Oset E, Weise W. *Nucl. Phys.* A319:477 (1979); *Nucl. Phys.* A329:365 (1979)
14. Hüfner J, Thies M. *Phys. Rev. C* 20:273 (1979)
15. Chiang HC, Hufner J. *J. Nucl. Phys.* A352: 442 (1981)
16. Girija V, Koltun DS. *Phys. Rev. Lett.* 52:1397 (1984)
17. Salcedo LL, Oset E, Vicente MJ, Garcia-Recio C. *Nucl. Phys.* A484:557 (1988)
18. Feshbach H. *Theoretical Nuclear Physics.* New York: Wiley (1992)
19. Thomas AW, Landau RH. *Phys. Rep.* 58: 121 (1980)
20. Kisslinger LS. *Phys. Rev.* 98:761 (1955)
21. Auerbach EH, Fleming DM, Sternheim MM. *Phys. Rev.* 162:1683 (1967)
22. Landau RH, Phatak SC, Tabakin F. *Ann. Phys.* 78:299 (1973)
23. Eisenstein RA, Miller GA. *Comput. Phys. Commun.* 8:130 (1974)
24. Celenza L, Liu LC, Shakin CM. *Phys. Rev. C* 12:1983 (1975); 13:2451 (1976)
25. Siciliano ER, Walker GE. *Phys. Rev. C* 13: 257 (1976)
26. Liu LC, Shakin CM. *Phys. Rev. C* 16:333 (1977)
27. Eisenstein RA, Tabakin F. *Comput. Phys. Commun.* 12:237 (1976)
28. Lee T-SH. *Phys. Lett.* 67B:282 (1977)
29. Johnson MB, Ernst DJ. *Ann. Phys.* 219:266 (1992); Chen CM, Ernst DJ, Johnson MB. *Phys. Rev. C* 47:R9 (1993)
30. Lee T-SH, Chakravarti S. *Phys. Rev. C* 16: 273 (1977)
31. Liu LC. *Phys. Rev. C* 17:1787 (1978)
32. Gmitro M, Kamalov SS, Mach R. *Phys. Rev. C* 36:1105 (1987)
33. Ericson M, Ericson TEO. *Ann. Phys.* 36: 323 (1966)
34. Striker K, McManus H, Carr JA. *Phys. Rev. C* 19:929 (1979); 22:2043 (1980)
35. Carr JA, McManus H, Stricker-Bauer K. *Phys. Rev. C* 25:952 (1982)
36. Ericson T, Weise W. *Pions and Nuclei.* Oxford, UK: Clarendon (1988)
37. Binon F, et al. *Nucl. Phys.* B17:168 (1970)
38. Binon F, et al. *Phys. Rev. Lett.* 35:145 (1975)
39. Binon F, et al. *Nucl. Phys.* A298:499 (1978)
40. Giulli S, Pilkuhn H, Schlaie HG. *Z. Phys. A* 302:42 (1981)
41. Piffaretti J, et al. *Phys. Lett.* 71B:324 (1977)
42. Arvieux J, et al. *Nucl. Phys.* A312:368 (1978); *Phys. Lett.* 76B:173 (1978)
43. Jansen J, et al. *Phys. Lett.* 77B:359 (1978)
44. Lunke C, et al. *Phys. Lett.* 78B:201 (1978)
45. Iverson S, et al. *Phys. Rev. Lett.* 40:17 (1978)
46. Ingram CHQ, et al. *Phys. Lett.* 76B:173 (1978)
47. Weiedner CA, et al. *Phys. Lett.* 78B:26 (1978)
48. Egger JP, et al. *Phys. Rev. Lett.* 39:1608 (1977)
49. Zeidman B, et al. *Phys. Rev. Lett.* 40:1539 (1978)
50. Blecher M, et al. *Phys. Rev. C* 20:1884 (1979)
51. Dytman SA, et al. *Phys. Rev. C* 19:971 (1979)
52. Preedom BM, et al. *Nucl. Phys.* A326:385 (1979)
53. Olmer C, et al. *Phys. Rev. C* 21:254 (1980)
54. Cottingame WB, Holtkamp DB. *Phys. Rev. Lett.* 45:1828 (1980)
55. Albanese JP, et al. *Nucl. Phys.* A350:301 (1980)
56. Wiedner CA, et al. *Phys. Lett.* 78B:26 (1980)
57. Johnson RR, et al. *Phys. Rev. Lett.* 43:844 (1979)
58. Barnett BM, et al. *Phys. Lett.* 97B:45 (1980)
59. Preedom BM, et al. *Phys. Rev. C* 20:1884 (1981)
60. Gretillat P, et al. *Nucl. Phys.* A364:270 (1981)

61. Dam SH, et al. *Phys. Rev. C* 25:2574 (1982)
62. Blecher M, et al. *Phys. Rev.* 28:2033 (1983)
63. Seestrom-Morris SJ, et al. *Phys. Rev. C* 28:1301 (1983)
64. Antonuk LE, et al. *Nucl. Phys.* A420:435 (1984)
65. Sobie RJ, et al. *Phys. Rev. C* 30:1612 (1984)
66. Leitch MJ, et al. *Phys. Rev. C* 29:561 (1984)
67. Boyer KG, et al. *Phys. Rev. C* 29:182 (1984)
68. Harvey CJ, et al. *Phys. Rev. C* 33:1454 (1986)
69. Oakley DS, et al. *Phys. Rev. C* 35:1392 (1987)
70. Tacik R, et al. *Phys. Rev. Lett.* 63:1784 (1989)
71. Nefkens BMK, et al. *Phys. Rev. C* 41:2770 (1990)
72. Pillai C, et al. *Phys. Rev. C* 43:1838 (1991)
73. Yen Y-F, et al. *Phys. Rev. Lett.* 66:1959 (1991)
74. Gorge JJ, et al. *Phys. Rev. Lett.* 66:2193 (1991)
75. Brinkmoller B, et al. *Phys. Rev. C* 44:2031 (1991)
76. Bartel J, Johnson MB, Singham M, Stocker W. *Phys. Rev. C* 49:2592 (1994)
77. Mathews SK, et al. *Phys. Rev. C* 51:2534 (1995)
78. Espy MA, et al. *Phys. Rev. C* 56:2607 (1997)
79. Hirata M, Lenz F, Yazaki K, Moniz EJ. *Ann. Phys.* 120:205 (1979)
80. Horikawa Y, Thies M, Lenz F. *Nucl. Phys.* A345:386 (1980)
81. Hirata M, Lenz F, Thies M. *Phys. Rev. C* 28:785 (1983)
82. Junker K, Karapiperis T, Kobayashi M. *Phys. Rev. C* 43:1911 (1991)
83. Lee T-SH, Ohta K. *Phys. Rev. C* 25:3043 (1982)
84. Betz M, Lee T-SH. *Phys. Rev. C* 23:375 (1981)
85. Rohlin J, et al. *Nucl. Phys.* B37:461 (1972)
86. McKeown RD, et al. *Phys. Rev. Lett.* 44: 1033 (1980); *Phys. Rev. C* 24:211 (1981)
87. Burleson GR, et al. *Phys. Rev. C* 21:1452 (1980)
88. Levenson SM, et al. *Phys. Rev. Lett.* 47:479 (1981); *Phys. Rev. C* 28:326 (1983)
89. Blecher M, et al. *Phys. Rev. C* 25:2554 (1982)
90. Baumgartner M, et al. *Nucl. Phys.* A399:451 (1983)
91. Ingram CH, et al. *Phys. Rev. C* 27:1578 (1983)
92. Aniol KA, et al. *Phys. Rev. C* 33:208 (1986)
93. Whitney RR, et al. *Nucl. Phys.* A408:417 (1983)
94. Klein A, et al. *Nucl. Phys.* A472:605 (1987)
95. Khandaker MA, et al. *Phys. Rev. C* 44:24 (1991)
96. Yuly M, et al. *Phys. Rev. C* 55:1848 (1997)
97. Thies M. *Nucl. Phys.* A382:434 (1982)
98. Chant NS, Roos PG. *Phys. Rev. C* 15:57 (1977); Rees L, Chant NS, Roos PG. *Phys. Rev. C* 26:1580 (1982)
99. Bowles TJ, et al. *Phys. Rev. C* 23:349 (1981)
100. Ashery D, et al. *Phys. Rev. Lett.* 50:482 (1983); *Phys. Rev. C* 30:946 (1984)
101. Dowell ML, et al. *Phys. Lett.* B344:91 (1995)
102. Park HT, et al. *Phys. Rev. C* 51:R1613 (1995)
103. Gregory NK, et al. *Phys. Rev. C* 58:3469 (1998)
104. Lehmann A, et al. *Phys. Rev. C* 60:024603 (1999)
105. Piasetzky E, et al. *Phys. Rev. Lett.* 46:1271 (1981); *Phys. Rev. C* 25:2687 (1982)
106. Kyle GS, et al. *Phys. Rev. Lett.* 52:974 (1984)
107. Gilad S, et al. *Phys. Rev. Lett.* 57:2637 (1986)
108. Hoibraten S, et al. *Phys. Rev. C* 43:1255 (1991)

109. Takaki T, Thies M. *Phys. Rev. C* 38:2230 (1988)
110. Wood SA, et al. *Phys. Rev. Lett.* 54:635 (1985)
111. Kinney ER, et al. *Phys. Rev. Lett.* 57:3125 (1986)
112. Gram PAM, et al. *Phys. Rev. Lett.* 62:1837 (1989)
113. Wood SA, et al. *Phys. Rev. C* 46:1903 (1992)
114. Vicente MJ, Oset E, Salcedo LL, Garcia-Recio C. *Phys. Rev. C* 39:209 (1989)
115. Lee HK, McManus H. *Nucl. Phys.* A167: 257 (1971)
116. Edward GW, Rost E. *Phys. Rev. Lett.* 26:785 (1971)
117. Lee T-SH, Tabakin F. *Nucl. Phys.* A226: 253 (1974)
118. Moore CF, et al. *Phys. Lett.* 80B:38 (1978)
119. Dehnhard D, et al. *Phys. Rev. Lett.* 43:109 (1979)
120. Bernstein AM, Brown VR, Madsen VA. *Phys. Rev. Lett.* 42:425 (1979)
121. Lee T-SH, Kurath D. *Phys. Rev. C* 21:293 (1980); *Phys. Rev. C* 22:1670 (1980)
122. Lee T-SH, Lawson RD. *Phys. Rev. C* 21:679 (1980)
123. Boyer KG, et al. *Phys. Rev. C* 24:598 (1981)
124. Seestrom-Morris SJ, Dehnhard D, Holtkamp DB, Morris CL. *Phys. Rev. Lett.* 46: 1447 (1981)
125. Seestrom-Morris SJ, et al. *Phys. Rev. C* 26:594 (1982)
126. Morris CL, et al. *Phys. Lett.* B108:172 (1982)
127. Morris CL, et al. *Phys. Rev. C* 35:1388 (1987)
128. Ritt S, et al. *Phys. Rev. C* 43:745 (1991)
129. Cohen S, Kurath D. *Nucl. Phys.* 73:1 (1965)
130. Millener DJ, Kurath D. *Nucl. Phys.* A255:315 (1975)
131. Gmitro M, Kvasil J, Mach R. *Phys. Rev. C* 31:1349 (1984)
132. Chakravarti S, et al. *Phys. Rev. C* 35:2197 (1987)
133. Lenz F, Thies M, Horikawa Y. *Nucl. Phys.* 140:266 (1982)
134. Nagaoka R, Ohta K. *Ann. Phys. (NY)* 184: 148 (1988)
135. Takaki T. *Ann. Phys.* 166:1 (1986)
136. Tanigichi S, Sato T, Ohtsubo H. *Prog. Theor. Phys.* 102:333 (1999)
137. Shamai Y, et al. *Phys. Rev. Lett.* 36:82 (1976)
138. Baer HW, et al. *Phys. Rev. Lett.* 45:982 (1980)
139. Baer HW, et al. *Phys. Rev. Lett.* 49:1376 (1982)
140. Bowman JD, et al. *Phys. Rev. Lett.* 50: 1195 (1983)
141. Doron A, et al. *Phys. Rev. C* 26:189 (1982)
142. Seth KK, et al. *Phys. Rev. Lett.* 43:1574 (1979)
143. Green SJ, et al. *Phys. Lett.* 88B:62 (1979)
144. Morris CL, et al. *Phys. Rev. Lett.* 45:1233 (1980)
145. Greene SJ, et al. *Phys. Rev. C* 25:927 (1982)
146. Seidl PA, et al. *Phys. Rev. Lett.* 50:1106 (1983)
147. Navon I, et al. *Phys. Rev. Lett.* 52:105 (1984)
148. Seidl PA, et al. *Phys. Rev. C* 30:973 (1984)
149. Altman A, et al. *Phys. Rev. Lett.* 55:1273 (1985)
150. Leith MJ, et al. *Phys. Rev. C* 54:1482 (1985)
151. Gilman R, et al. *Phys. Rev. C* 33:1082 (1986)
152. Leitch MJ, et al. *Phys. Rev. C* 39:2356 (1989)
153. Miller, GA, Spencer JE. *Phys. Lett.* 53: 329 (1974); *Ann. Phys. (NY)* 100:562 (1976)
154. Miller GA. *Phys. Rev. C* 24:221 (1981)
155. Saharia A, Woloshyn RM. *Phys. Lett.* 84B:401 (1979)
156. Landau RH, Thomas AW. *Phys. Lett.* 88B: 226 (1979)
157. Liu LC. *Phys. Rev. C* 23:814 (1981)

158. Polyzou WN, Gibbs WR, Stephenson GJ. *Phys. Rev. C* 23:2648 (1981)
159. Kaufmann WB, Gibbs WR. *Phys. Rev. C* 28:1286 (1983)
160. Saharia AN, Woloshyn RM. *Phys. Rev. C* 21:1111 (1980)
161. Hirara M. *Phys. Rev. C* 24:1604 (1981)
162. Oset E. *Nucl. Phys.* A356:413 (1981)
163. Chakravarti S. *Phys. Lett.* 90B:350 (1980)
164. Johnson MB, Siciliano ER. *Phys. Rev. C* 27:1647 (1983)
165. Kagarlis MA, Johnson MB, Fortune HT. *Ann. Phys. (NY)* 240:56 (1995)
166. Siciliano E, Johnson MB. *Ann. Phys.* 203: 1 (1990)
167. Lee T-SH, Kurath D, Zeidman B. *Phys. Rev. Lett.* 39:1307 (1977)
168. Li G-L, Li C-H, Lee T-SH. *Phys. Lett.* 99B:200 (1981)
169. Auerbach N, Gibbs WR, Ginocchio JN, Kaufmann WB. *Phys. Rev. C* 38:1277 (1988)
170. Karapiperis T, Kobayashi M, Hirata M. *Phys. Lett.* 144B:23 (1984)
171. Karapiperis T, Kobayashi M. *Phys. Rev. Lett.* 54:1230 (1985)
172. Miller GA. *Phys. Rev. Lett.* 53:2008 (1984)
173. Bilger R, Clement HA, Schepkin MG. *Phys. Rev. Lett.* 71:42 (1993)
174. Jiang MF, Koltun DS. *Phys. Rev. C* 42: 2662 (1990)
175. Johnson MB, et al. *Phys. Rev. C* 44:2480 (1991)
176. Liu LC, Franco V. *Phys. Rev. C* 11:760 (1975)
177. Oset E, Strottman D, Brown GE. *Phys. Lett.* 73B:393 (1978)
178. Bleszynski M, Glauber RJ. *Phys. Rev. Lett.* 60:1483 (1988)
179. Mutazz N, et al. *Phys. Rev. C* 58:2292 (1998)
180. Ashery D, et al. *Phys. Rev. C* 23:2173 (1981)
181. Altman A, et al. *Phys. Rev. Lett.* 50:1187 (1983)
182. Backenstoss G, et al. *Phys. Rev. Lett.* 55: 2782 (1985)
183. Altman A, et al. *Phys. Rev. C* 34:1757 (1986)
184. Aniol K, et al. *Phys. Rev. C* 33:1714 (1986)
185. Burger W, et al. *Phys. Rev. Lett.* 57:58 (1986)
186. Schumacher RA, et al. *Phys. Rev. C* 38: 2205 (1988)
187. Backenstoss G. et al. *Phys. Rev. Lett.* 61: 923 (1988)
188. Backenstoss G, et al. *Phys. Lett.* B222:7 (1989)
189. Burger W, et al. *Phys. Rev. C* 41:2215 (1990)
190. Steinacher M, et al. *Nucl. Phys.* A517:413 (1990)
191. Mukhpadhyay S, et al. *Phys. Rev. C* 43: 957 (1991)
192. Weber P, et al. *Nucl. Phys.* A534:541 (1991)
193. Adimi F, et al. *Phys. Rev. C* 45:2589 (1992)
194. Hyman SD, et al. *Phys. Rev. C* 47:1184 (1993)
195. Alteholz T, et al. *Phys. Rev. Lett.* 73:1336 (1994)
196. Alteholz T, et al. *Nucl. Instrum. Methods A* 373:374 (1996)
197. Ashery D, et al. *Phys. Rev. Lett.* 47:895 (1981)
198. Backenstoss G, et al. *Phys. Lett.* B137:329 (1984)
199. Baumgartner M, et al. *Nucl. Phys.* A399: 451 (1983)
200. Gotta P, et al. *Phys. Lett.* B112:129 (1982)
201. Ingram CHQ, et al. *Phys. Rev. C* 27:1548 (1983)
202. Androic D, et al. *Phys. Rev. C* 53:R2591 (1996)
203. Lehmann A, et al. *Phys. Rev. C* 55:2931 (1997)
204. Lehmann A, et al. *Phys. Rev. C* 56:1872 (1997)
205. Mateos A, et al. *Phys. Rev. C* 58:942 (1998)

206. McKeown R. et al. *Phys. Rev. Lett.* 44: 1033 (1980)
207. Moinester MA, et al. *Phys. Rev. Lett.* 52:1203 (1984)
208. Ritchie BG. *Phys. Rev. C* 28:926 (1983)
209. Ritchie BG. *Phys. Rev. C* 44:533 (1991)
210. Rowntree D, et al. *Phys. Rev. C* 60:054610 (1999)
211. Kotlinski B, et al. *Eur. Phys. J. A* 1:435 (1998)
212. Ohta K, Thies M, Lee T-SH. *Ann. Phys.* 163:420 (1985)
213. Brown GE, Toki H, Weise W, Wirzba A. *Phys. Lett.* 118B:39 (1982)
214. Schmacher RA, et al. *Phys. Rev. C* 38: 2205 (1988)
215. Mack DJ, et al. *Phys. Rev. C* 45:1767 (1992)
216. Chant NS, Roos PG. *Phys. Rev. C* 39:957 (1989)
217. Wilkin C, et al. *Nucl. Phys.* B62:61 (1973)
218. Clough AS, et al. *Nucl. Phys.* B76:15 (1974)
219. Jaeckle R, Pilkuhn H, Schlaile HG. *Phys. Lett.* B76:177 (1978)
220. Jeppesen RH, et al. *Phys. Rev. C* 27:697 (1983)
221. Tacik R, et al. *Phys. Rev. C* 57:1295 (1998)
222. Gianelli RA, et al. *Phys. Rev. C* 61: 054615-1 (2000)
223. Lipkin HJ, Lee T-SH. *Phys. Lett.* 183:22 (1987)
224. Lee T-SH. *Proc. Second Workshop Electronucl. Phys. with Internal Targets and the BLAST Detector*, ed. R Alarcon, R Milner, p. 39. Singapore: World Sci. (1999)
225. Lipari P. Summary talk in *Proc. First Int. Workshop on Neutrino-Nucleus Interact. in the Few GeV Region, KEK, Jpn., Dec. 13–16, 2001*. (2002) In press
226. Pieper SC, Wiringa RB. *Annu. Rev. Nucl. Part. Sci.* 51:53 (2001)
227. Lee T-SH, Wiringa RB. *Phys. Rev. C* 63: 014006 (2001)